Am J Transl Res 2023;15(11):6381-6403
www.ajtr.org /ISSN:1943-8141/AJTR0152930

Original Article

Ameliorative effects of allogeneic and xenogenic bone marrow-derived mesechymal stem cells on carbon tetrachloride-induced rat liver injury and cirrhosis via modulation of oxidative stress, apoptosis, inflammation, and Nrf2 expression

Asmaa A Abdel Fattah[1], Manal Abdul-Hamid[1], Taghreed N Almanaa[2], Lama A Alhaber[2], Samraa H Abdel-Kawi[3], Fatma El-Zahraa S Abdel Rahman[4], Osama M Ahmed[5]

[1]Division of Cell Biology, Histology and Genetics, Department of Zoology, Faculty of Science, Beni-Suef University, Beni-Suef 62511, Egypt; [2]Department of Botany and Microbiology, College of Science, King Saud University, Riyadh 11451, Saudi Arabia; [3]Department of Histology, Faculty of Medicine, Beni-Suef University, Beni-Suef 62521, Egypt; [4]Department of Basic Sciences, Faculty of Oral and Dental Medicine, Nahda University, Beni-Suef 62764, Egypt; [5]Division of Physiology, Department of Zoology, Faculty of Science, Beni-Suef University, Beni-Suef 62521, Egypt

Received August 14, 2023; Accepted October 26, 2023; Epub November 15, 2023; Published November 30, 2023

Abstract: Objectives: The aim of this study was to compare the effects of bone marrow-derived mesenchymal stem cells (BM-MSCs) isolated from mice (xenogeneic) and rats (allogeneic) on liver injury induced by carbon tetrachloride (CCl4) as well as to explore the modulatory effects on of oxidative stress, apoptosis, inflammation, and Nrf2 expression. Methods: Male Wistar rats were intraperitoneally injected with CCl4 (0.5 mL/kg) twice a week for 8 weeks. The animals were intravenously infused with BM-MSCs isolated from male mice or rats (1×10^6 cells/rat/week) into the lateral tail vein for 4 weeks. Results: The treatment with BM-MSCs produced a significant increase in the diminished serum albumin level, a significant decrease in liver lipid peroxidation and an increase in glutathione content as well as SOD, GST, and GPx activities. Furthermore, BM-MSCs from both mice and rats produced a significant decrease in the elevated mRNA expression of liver CYP1A1, MMP-9, procollagen α1, TGF-β1, and increase in expression of lowered IL-4, IL-10, cluster CD-105, and Oct3/4. In liver of CCl4-injected rats, the lower protein expression of Nrf2 was upregulated and higher expressions of caspase-3, TNF-R1, NF-κB p65, TNF-α, p53, and COX-2 were downregulated by mice and rats' BM-MSCs. Histologically, BM-MSCs from both mice and rats successfully improved liver structural integrity and protected against liver injury. Conclusions: The rats-derived BM-MSCs were significantly more potent than mice-derived BM-MSCs. Mice BM-MSCs and rats' BM-MSCs acted to improve CCl4-impaired liver function, structural integrity, fibrosis and cirrhosis in male Wistar rats *via* the suppression of oxidative stress, inflammation, and apoptosis and the enhancement of the antioxidant defense system.

Keywords: CCl4, rats, liver cirrhosis, bone marrow mesenchymal stem cells, oxidative stress, apoptotic markers, inflammatory cytokines

Introduction

Around 750,000 new cases of liver cancer are reported each year worldwide. The majority of people who get hepatocellular carcinoma (HCC) die from it, according to population-based interventions, because the liver cancer cure rate is still very low. Data show that five-year survival rates in the United States of America (USA) have marginally increased to around 26% [1].

Carbon tetrachloride (CCl4) has been known to produce acute and chronic tissue damage and liver toxicity [2]. The injury caused by CCl4 to hepatocytes is distinguished by centrilobular necrosis followed by hepatic fibrosis [3, 4]. CCl4-induced hepatotoxicity in the animal mod-

els is due to the lipid peroxidation (LPO), which is thought to be harmful in other tissues as well [5]. Cirrhosis often begins with chronic hepatocyte damage, which in turn triggers a sequence of complicated cell-to-cell and cell-to-matrix interactions and, finally, activates hepatic stellate cells, the principal producers of excessive collagen during the cirrhosis process [6].

Oxidative stress and inflammation play crucial implications in several ailments, including liver toxicity [7]. Although the carcinogenic mechanism for CCl4-induced liver cancer is not fully understood, there is accumulating evidence that CCl4-induced cytotoxicity depends on oxidative stress caused by CCl4-induced generation of reactive oxygen species (ROS) [8]. The formation of ROS leads to cellular damage, DNA fragmentation, degeneration of nuclear protein, dysfunction and, finally, programmed cell death (apoptosis) [9].

In a healthy liver, myeloid-derived suppressor cells (MDSCs) exist [10], and they grow in a chronic liver illness [11]. By producing the immunosuppressive chemicals IL-10, TGF-β, and arginase, MDSCs are able to inhibit T-cell activation [12]. It is believed that granulocytic cells, like neutrophils, are mostly missing from a healthy liver and only build up in reaction to infection and inflammation [13]. The adult healthy liver possesses an active and complex cytokine milieu, which includes basal levels of both pro-inflammatory and anti-inflammatory cytokines (IL-2, IL-7, IL-12, IL-15, and interferon (IFN)-γ) [14, 15].

MSCs represent a stem cell source with great promise in regenerative medicine. MSCs were proven to develop into hepatocytes *in vitro* [16, 17] and *in vivo* [16, 17]. MSCs could also help heal damaged lungs, livers, and hearts by lowering inflammation, collagen deposition, and remodeling [18-21]. MSCs may be able to not only repair damaged tissue but also reduce persistent fibrogenesis. Despite claims that bone marrow or MSCs can diminish CCl4-induced liver fibrosis in rats, the underlying mechanism remains to be fully elucidated, and the supporting evidence is debated [20, 22]. While delaying MSCs administration by 1 week after CCl4 challenge eliminated the ability to prevent disease progression [20], a 4-week bone marrow therapy of CCl4-induced liver disease did significantly reduce liver fibrosis in rats [22, 23]. Moreover, further studies are required to compare the effects of allogeneic and xenogeic MSCs liver injury and cirrhosis.

Consequently, the presented study aimed to evaluate the ability of MSCs derived from rats and mice bone marrow to repair liver tissue afflicted by CCl4-induced cirrhosis using biochemical and molecular biology assays as well as histological, immunohistochemical and ultrastructural investigations.

Materials and methods

Experimental animals

Male Wistar rats, weighing 120 ± 10 g and aged 7-8 weeks were obtained from the Helwan Station of VACSERA (the Egyptian Organization for Biological Products and Vaccines). Prior to the start of the experiment, rats were kept under observation for a week. The animals were kept in polypropylene cages in a controlled environment with a daily normal light/dark cycle of 12 hours and a temperature of 22 ± 2°C. Tap water and a typical pellet feed were accessible to the animals at all times. The rats were sacrificed at the end of the experiment by breathing light diethyl ether anesthesia. The guidelines and instructions of the Experimental Animal Ethics Committee, Faculty of Science, Beni-Suef University, Egypt for the use and care of animals were followed in all animal procedures (Ethical Approval Number: BSU/FS/2019-73). Every effort was made to minimize the number of animals and their suffering.

Isolation, culture and propagation of MSCs from bone marrow

The isolation, culture and propagation of bone marrow-derived MSCs (BM-MSCs) were carried out according to the methods of Chaudhary and Rath [24] and Ahmed [25]. Femurs and tibiae were dissected out and the associated connective tissues were removed after decapitating rats by cervical dislocation and sterilizing the external body surface with 70% (vol/vol) ethanol. Each bone's epiphysis was sliced using sterile scissors while operating in laminar flow, and BM cells were then extracted and centrifuged at 3000 rpm for 5 minutes at room temperature in a 15 mL polypropylene tube. In DMEM supplemented with FBS, sodium hydrogen carbonate, and an antibiotic/antimycotic solution in ratios of 15%, 0.36%, and 1% respectively, the pellet was washed and sus-

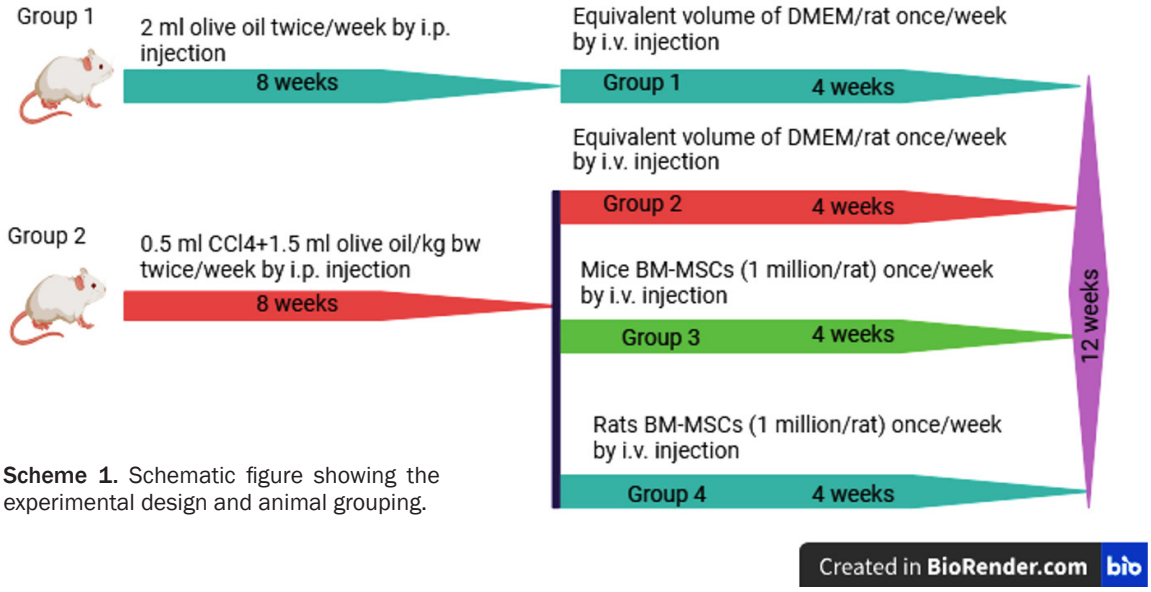

Scheme 1. Schematic figure showing the experimental design and animal grouping.

pended. To check viability, cells were stained with 0.4% trypan blue solution and were then counted by using haemocytometer and inverted microscope at 100× magnification. Histological, immunohistochemical and ultrastructural features were also investigated. Cells (25 × 10^6) were seeded in T-25 cm^2 canted cell culture flasks with a density about 1 × 10^6 cells/cm^2 area and then kept at 37°C in 5% CO_2 humidified incubator, with the non-adherent, floating, and dead cells removed each 4 days during the 10 days of culture. Following two pre-warmed (37°C) PBS washes, the adherent cells were trypsinized with 1.0 mL to 2.0 mL of pre-warmed 0.25% trypsin/1 mM EDTA at 37°C for 2-3 min. Cells were collected, spun at 3000 rpm for 5 min in a 15 mL polypropylene tube, counted, and their viability assessed by trypan blue staining after trypsin activity was suppressed by adding 2-3 mL of full culturing solution. Finally, the morphology of the MSCs was described using an inverted microscope to validate their identification.

Animal grouping

The adult male Wistar rats of this study were allocated into two groups. Group one contained 6 rats and group 2 contained 18 rats and they were then divided into 3 subgroups with each group containing 6 rats. The grouping was designed as follow (**Scheme 1**):

Group I (Control); the rats of this group were given olive oil (2 mL/kg body weight (b.w.)) twice a week for 8 weeks by intraperitoneal (i.p.) injection and they were then given DMEM once a week into the lateral tail vein for 4 weeks.

Group II (CCl4); the rats of this group were given the CCl4 (0.5 mL/kg) [26] mixed with olive oil (1.5 mL/kg) twice a week by i.p. injection for 8 weeks and they were then given DMEM once a week into the lateral tail vein for 4 weeks.

Group III (CCl4+mice BM-MSCs); the rats of this group were given CCl4 (0.5 mL/kg) mixed with olive oil (1.5 mL/kg) twice a week by i.p. injection for 8 weeks and they were then given mice BM-MSCs (1 × 10^6 cell/rat) once a week into the lateral tail vein for 4 weeks [27].

Group IV (CCl4+rats' BM-MSCs); the rats of this group were given CCl4 (0.5 mL/kg) mixed with olive oil (1.5 mL/kg) twice a week by i.p. injection for 8 weeks and they were then given rat BM-MSCs (1 × 10^6 cell/rat) once a week into the lateral tail vein for 4 weeks [27].

Rats were anaesthetized with diethyl ether inhalation before they were put to death by cervical dislocation at the end of the experiment. Blood samples were drawn from the jugular vein using gel and clot activator tubes, and they were centrifuged at 3000 rpm for 15 minutes. The supernatant sera were quickly aspirated, divided into three aliquots for each individual animal, and kept at -70°C until needed for additional analysis. Rats were dissected, and the livers were removed and placed in sterile isotonic saline. For histological analysis, 3 mm^3 pieces of liver were fixed in 10% neutral-buff-

Table 1. Sequences of primers of various rat genes used for qRT-PCR

Gene	Primer sequence	Ref.
β-Actin	F 5'-TGTTTGAGACCTTCAACACC-3' R 5'-CGCTCATTGCCGATAGTGAT-3'	[38]
Procollagen α-1	F 5'-TCACCTACAGCACGCTTG-3' R 5'-GGTCTGTTTCCAGGGTTG-3'	[39]
MMP-9	F 5'-CCACCGAGCTATCCACTCAT-3' R 5'-GTCCGGTTTCAGCATGTTTT-3'	[40]
IL-4	F 5'-ACCTTGCTGTCACCCTGTTCTGC-3' R 5'-GTTGTGAGCGTGGACTCATTCACG-3'	[41]
IL-10	F 5'-TGCCAAGCCTTGTCAGAAATGATCAAG-3' R 5'-GTATCCAGAGGGTCTTCAGCTTCTCTC-3'	[41]
Oct3/4	F 5'-CGGGCTGATGGGCAAGTT-3' R 5'-GGGCAGGAAGGATGGGTAA-3'	[42]
TGF-β1	F 5'-TTG CCC TCT ACA ACC AAC ACA A-3' R 5'-GGC TTG CGA CCC ACG TAG TA-3'	[43]
CYP1a1	F 5'-TAACTCTTCCCTGGATGCCTTCAA-3' R 5'-GTCCCGGATGTGGCCCTTCTCAAA-3'	[44]
UGT1A	F 5'-TTGGTGGGATAAACTGCCTTCA-3' R 5'-GAATTCTGCCCAAAGCCTCA-3'	[45]
CD-105	F 5'-CCCCCGTACGTCTCCTGGCTCATC-3' R 5'-GGGGTGTGTCTGGGAGCTCGAA-3'	[46]

ered formalin (NBF). Before being employed for quantitative real time-polymerase chain reaction (qRT-PCR) and Western blotting studies, additional fragments were temporarily kept in sterile Eppendorf tubes at -70°C. The other liver tissue from each rat was likewise temporarily stored in a deep freezer at -70°C while the antioxidant defense system and oxidative stress indicators were estimated.

Biochemical tests for liver functions

Alanine transaminase (ALT) and aspartate transaminase (AST) activities were detected using kinetic reagent kits purchased from Human Company, Max-planck- Ring 21.65205 Wiesbaden (Germany) according to Schumann and Klauke [28]. Alkaline phosphatase (ALP) activity in serum was estimated using a kinetic reagent kit purchased from Biotec Diagnostics Company (Bristol, UK, BS39 5BX) according to the method of TIETZ [29]. Serum gamma-glutamyl transferase (γ-GT) activity was assayed using kinetic reagent kit obtained from Biotec Diagnostics Company based on the method of Tietz [30]. Direct and total bilirubin concentrations were determined based on the method of Jendrassik and Grof [31] using reagent kits purchased from Diamond Diagnostics Company (Cairo, Egypt). Serum albumin level was determined according to the method of Gendler [32] using reagent kits purchased from Spinreact Company (Santa Coloma, Spain).

Oxidant and anti-oxidant defense biomarkers of liver

Malondialdehyde (MDA) level, as a measure for the extent of lipid peroxidation (LPO), was assayed based on the approach of Yagi [33]. Marklund and Marklin's approach was used to measure superoxide dismutase (SOD) activity, while Beutler's method was used to measure glutathione (GSH) concentration using dithiobis-2-nitrobenzoic acid (DTNB) [34, 35]. Glutathione peroxidase (GPx) activity was assessed using the method of Matkovics [36] with some changes, and glutathione transferase (GST) activity was assessed using the method of Mannervik and Guthenberg [37].

qRT-PCR analysis

The mRNA levels of TGF-β1 (transforming growth factor-beta 1), procollagen α-1, MMP-9 (matrix metalloproteinase-9), IL-4 (interleukin-4), IL-10 (interleukin-10), Oct3/4 (octamer-binding transcription factor 3/4), CYP1a1 (cytochrome P450 family 1 subfamily A polypeptide 1), and UGT1A (uridine diphospahte-glucuronosyl transferase 1A) (**Table 1**) were quantified by qRT-PCR analysis. The messenger ribonucleic acid (mRNA) levels for MSC specific genes of lymphocyte common antigens cluster differentiation-45 (CD-45) and CD-105 were also estimated by qRT-PCR. In brief, total ribonucleic acid (RNA) was isolated from the rat livers using Trizol Reagent (Invitrogen, Grand Island, NY, USA) in accordance with the manufacturer's manual. Cloned deoxyribonucleic acid (cDNA) was created using the PrimeScript RT Master Mix reagent kit from Takara (Dalian, China), in accordance with the manufacturer's instructions. Premix Ex reagent kit (Takara, Dalian, China) was used to create real-time qRT-PCR reactions, which were then carried out using an automated ABI ViiATM 7 real-time PCR system (Applied Biosystems, Waltham, MA, USA).

Western blotting analysis

Each homogenized tissue sample was treated using the Ready Prep TM protein extraction kit (total protein) provided by Bio-Rad Inc. (Catalogue #163-2086; USA) in accordance with the manufacturer's instructions. The Bradford Protein Assay Kit (SK3041) was developed by Bio Basic Inc. (Markham, Ontario, Canada) for quantitative protein analysis. Each sample was subjected to a Bradford assay, performed in accordance with the manufacturer's recommendations. The samples were divided using SDS-PAGE (sodium dodecyl sulphate poly acrylamide gel electrophoresis), a common method for dividing proteins according to their molecular weight. The manufacturer's instructions were followed while creating the SDS-PAGE TGX Stain-Free Fast Cast. Several primary antibodies were employed, including those against cleaved caspase-3, TNF-R1, Nrf2, and NF-κB p65. In accordance with manufacturer's recommendations, primary antibody was diluted in tris-buffered saline with Tween 20 (TBST). Each primary antibody solution was incubated at 4°C overnight with the blotted target protein. The blot was rinsed with TBST 3-5 times for 5 minutes. The blotted target protein was incubated for 1 hour at room temperature in a horseradish peroxidase (HRP)-conjugated secondary antibody (goat anti-rabbit IgG-HRP-1 mg goat mab - Novus Biologicals) solution. The blot was rinsed with TBST 3-5 times for 5 minutes. According to the manufacturer's instructions, the chemiluminescent substrate (Clarity TM Western ECL substrate, Bio-Rad cat#170-5060; USA) was applied to the blot. A CCD camera-based imager was used to record the chemiluminescent signals. The target proteins' band intensities were compared to the control sample β-actin (a housekeeping protein) using image analysis software on the ChemiDoc MP imager.

Histological examinations of liver tissue

Animals were dissected to remove the liver at the end of the experiment after being anaesthetized with light diethyl ether for the histology preparations. Liver was cut into small pieces of 3 mm^3 and then fixed in 10% NBF for 24 h. Sections of 4-5 μm in thickness were prepared with a microtome and stained with haematoxylin & eosin (H&E) and Masson's trichrome (MT) for histopathological studies [47, 48]. To look for histological lesions, stained liver sections were examined. Lesions or injuries were rated as absence (0), mild (I), moderate (II), and severe (III) for changes, respectively, in three randomly chosen fields of each section (100) [49]. For changes of less than 30%, 30-50%, and more than 50%, the corresponding grades were 0%, 30-50%, and more than 50%. The graded lesions included steatosis or fatty changes, vacuolar degeneration, vascular congestion, binuclear hepatocytes, necrosis and collagen fibers.

Immunohistochemical study

Immunolocalization for TNF-α (tumor necrosis factor-α), p53 (apoptotic protein 53) and COX-2 (cyclooxygenase-2) was performed on 5-6 μm thickness liver slices and stained with the streptavidin-biotin-peroxidase staining technique [50]. After being deparaffinized in xylene, slices were rehydrated in descending alcohol grades. To block endogenous peroxidase and non-specific antibody binding sites, the sections were treated with 0.3 percent hydrogen peroxide for 20 minutes at room temperature and 5 percent normal bovine serum (1:5 diluted TRIS) for 20 minutes at room temperature, respectively. To lessen non-specific binding, the slices were washed in phosphate buffered saline and 10% normal goat serum. The sections were treated for 1 hour with anti-sera from Bio Genex (Santa Cruz, CA, USA) that contained primary antibodies for rat TNF-α, p53, and COX-2. For immunolabelling, the sections were incubated for 30 minutes with a biotinylated secondary antibody (Dako-K0690; Dako Universal LSAB Kit), streptavidin horseradish peroxidase (Dako-K0690), and 3, 30-diaminobenzidine tetrahydrochloride substrate kit (Sigma-D5905; Sigma-Aldrich Company Ltd., Gillingham, UK). Final steps included staining the nuclei using Harry's hematoxylin stain, drying them in graded alcohol, clearing them in xylene, and mounting them in dibutylphthalate polystyrene xylene (DPX). A high-power light microscope was used to examine the antibodies' binding to determine its effectiveness.

Evaluation of staining intensity by image J analysis

Using the "Leica Quin500C" image analyzer computer system, cells were examined on three slides of each group to measure the area per-

Table 2. Effect of rats' BM-MSCs and mice BM-MSCs on liver function parameters in serum of CCL4-injected rats

Groups	ALT (U/L)	AST (U/L)	ALP (U/L)	γ-GT (U/L)	Direct Bilirubin (mg/dL)	Total Bilirubin (mg/dL)	ALB (g/dL)
Normal Control	50.94 ± 2.29[a]	152.78 ± 15.29[a]	313.73 ± 14.60[a]	4.28 ± 0.19[a]	0.12 ± 0.01[a]	0.40 ± 0.01[a]	3.28 ± 0.08[d]
CCl4	92.38 ± 5.43[c]	236.05 ± 7.89[b]	855.92 ± 10.12[d]	7.79 ± 0.17[c]	0.54 ± 0.01[d]	1.31 ± 0.02[d]	1.32 ± 0.04[a]
CCl4/mice BM-MSCs	70.60 ± 7.71[b]	185.43 ± 5.74[a]	642.27 ± 21.46[c]	5.82 ± 0.15[b]	0.43 ± 0.02[c]	0.68 ± 0.02[c]	1.93 ± 0.09[b]
CCl4/rats BM-MSCs	59.62 ± 2.52[a,b]	159.12 ± 13.12[a]	546.32 ± 11.08[b]	4.70 ± 0.21[a]	0.19 ± 0.01[b]	0.53 ± 0.02[b]	2.61 ± 0.10[c]

Data are represented as mean ± SE. Number of animals in each group is six. Mean values with different superscript letters are significantly different at $P < 0.05$. a, b, c, d indicated the difference or similarity between groups.

centage of positive TNF-α, p53 and COX-2 immuno-reactive cells in the liver (Leica Imaging System Ltd., Cambridge, England).

Electron microscopic study

Liver samples were divided into 1 mm^3 pieces and immediately fixed in 3% fresh glutraldehyde-formaldehyde at 4°C for 18-24 h. Following a phosphate buffer wash (pH 7.4), the specimens were post-fixed in isotonic 1% osmium tetroxide for an hour at 4°C. Alcoholic serial dehydration was performed. The procedure for embedding the specimens in Spur resin began with passing the specimens through a mixture of propylene oxide and resin, followed by a mixture of propylene oxide and resin at a ratio of 1:3 overnight, before being transferred to capsules containing fresh resin and baked for a day at 60°C to produce hard blocks. To identify the area of interest, semi-thin slices were cut at 1.0 m thickness using an ultracut Reichert-Jung ultra-microtome, stained with toluidine blue, and then viewed under a light microscope. Subsequently, using the ultramicrotome glass knives, ultrathin slices were created. They were subsequently stained with uranyl acetate and lead citrate [51] and analyzed using a Joel CX 100 transmission electron microscope run at an accelerating voltage of 60 KV.

Statistical analysis

The collected data were shown as mean ± standard error (SE). The number of animals in each group was six. The Statistical Package of Social Sciences (SPSS) (Cary, NC, USA) version 21 was used for the statistical analysis. The data was analyzed by one-way analysis of variance (ANOVA) followed by Duncan's multiple range testing [52, 53] to compare various groups with each other. Values were considered significant at $P < 0.05$.

Results

Of BM-MSCs on CCl4-induced liver dysfunction

As summarized in **Table 2**, ALT, AST, ALP, and γ-GT activities, as well as direct and total bilirubin levels, were significantly ($P < 0.05$) higher in CCl4-injected rats than those in the normal control group. However, these levels were significantly ($P < 0.05$) decreased by the injection of rats and mice BM-MSCs. In contrast, albumin levels were significantly ($P < 0.05$) lower in the CCl4-injected group than those in the control group but significantly ($P < 0.05$) increased upon the injection of rats and mice BM-MSCs.

Liver parameters of oxidant and antioxidant defense

Injection of rats and mice BM-MSCs caused significant elevation of liver LPO levels (**Table 3**). In contrast, CCl4-injection produced a significant decrease in the liver levels of antioxidant parameters, including GSH levels and GPx, GST, and SOD activities, below those of the normal control. Moreover, the injection of rats and mice BM-MSCs in CCl4-injected rats significantly prevented the CCl4-induced elevation of liver LPO levels and suppression of the above antioxidant parameters.

Histopathological result of liver tissue

Both routine staining with H&E and special staining with Masson's Trichrome for collagen fibers were applied to describe liver histopathological changes.

H&E staining

Histopathological analysis of hematoxylin and eosin-stained sections of liver tissue revealed normal central vein, sinusoids, and hepatocytes in the control animals (**Figure 1A**). However, in the liver of CCl4-treated animals, hepat-

Table 3. Effect of on oxidative stress and anti-oxidant defense system

Groups	LPO (nmol MDO/100 mg tissue)	SOD (U/mg tissue)	GSH (nmol/100 mg tissue)	GST (U/100 mg tissue)	GPx (mU/100 mg tissue)
Normal Control	25.88 ± 0.57[a]	105.32 ± 2.08[d]	18.68 ± 0.74[c]	165.77 ± 1.21[d]	149.09 ± 1.76[d]
CCl4	77.36 ± 1.18[d]	41.02 ± 1.77[a]	5.00 ± 0.32[a]	98.82 ± 0.64[a]	111.44 ± 0.24[a]
CCl4/mice BM-MSCs	52.57 ± 0.67[c]	56.02 ± 0.74[b]	6.36 ± 0.27[a]	111.09 ± 1.44[b]	123.10 ± 0.64[b]
CCl4/rats BM-MSCs	35.03 ± 1.92[b]	85.00 ± 2.07[c]	11.52 ± 0.41[b]	141.69 ± 0.87[c]	135.13 ± 1.02[c]

Data are represented as mean ± SE. Number of animals in each group is six. Mean values with different superscript letters are significantly different at $P < 0.05$. a, b, c, d indicated the difference or similarity between groups.

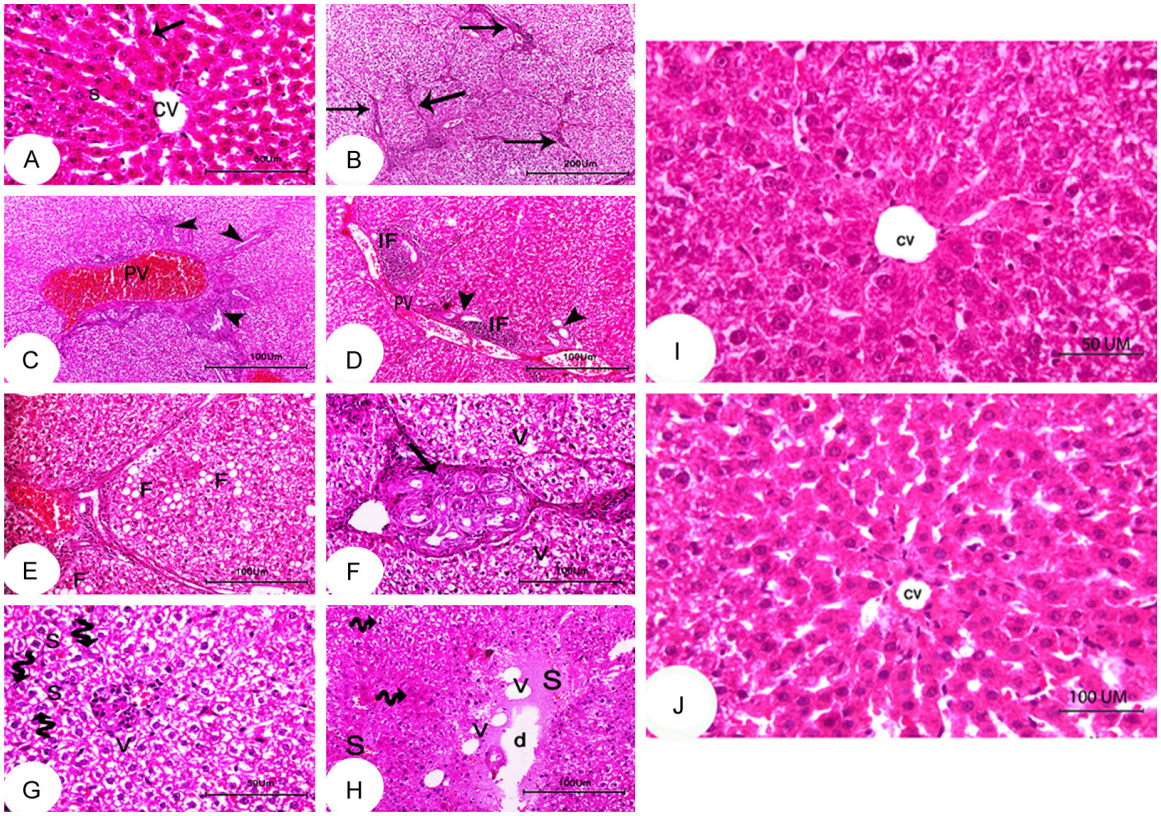

Figure 1. Photomicrographs of liver section of control group. (A) Central vein (CV), sinusoids (S) and hepatocyte (arrow) (Scale bars of A = 50 μm). (B) Liver section of CCl4-treated group showing hepatic nodules surrounded by fibrous tissues (arrows) (Scale bars of B = 200 μm). (C, D) Liver section of CCL4-treated group showing portal area containing dilated congested portal vein (PV), marked proliferative bile ducts (arrow heads) and mononuclear leukocyte infiltration (IF) (Scale bars of C, D = 100 μm). (E) Liver section of CCl4-treated group showing fatty changes of hepatocytes (F) (Scale bars of E = 100 μm). (F-H) Liver section of CCl4-treated group revealing abnormal aggregations of proliferated bile ductule (arrow) surrounded by thick membrane, vacuolated cytoplasm (V), dilated hyperemic sinusoids (S), dissolution of cytoplasm (d) and marked increase of bi-nucleated hepatocytes (wave arrow) (Scale bars of F, G = 50 μm, Scale bars of H = 100 μm). Photomicrographs of liver section of treated groups (I) CCl4/mice BM-MSCs and (J) CCl4/rats' BM-MSCs demonstrating amelioration of architecture of the hepatocytes, sinusoids, and central vein (CV) (H&E stain; Scale bars of A = 50 μm, Scale bars of B = 100 μm).

ic nodules were surrounded by fibrous tissues (**Figure 1B**), the portal vein was dilated and congested, and a proliferation of bile ducts and mononuclear leukocyte infiltration were seen in the portal area (**Figure 1C**, **1D**). Hepatocytes exhibited fatty changes (**Figure 1E**), vacuolations and dissolution of cytoplasm, and a marked increase of bi-nucleation, with dilated hyperemic sinusoids in the surround (**Figure 1F-H**).

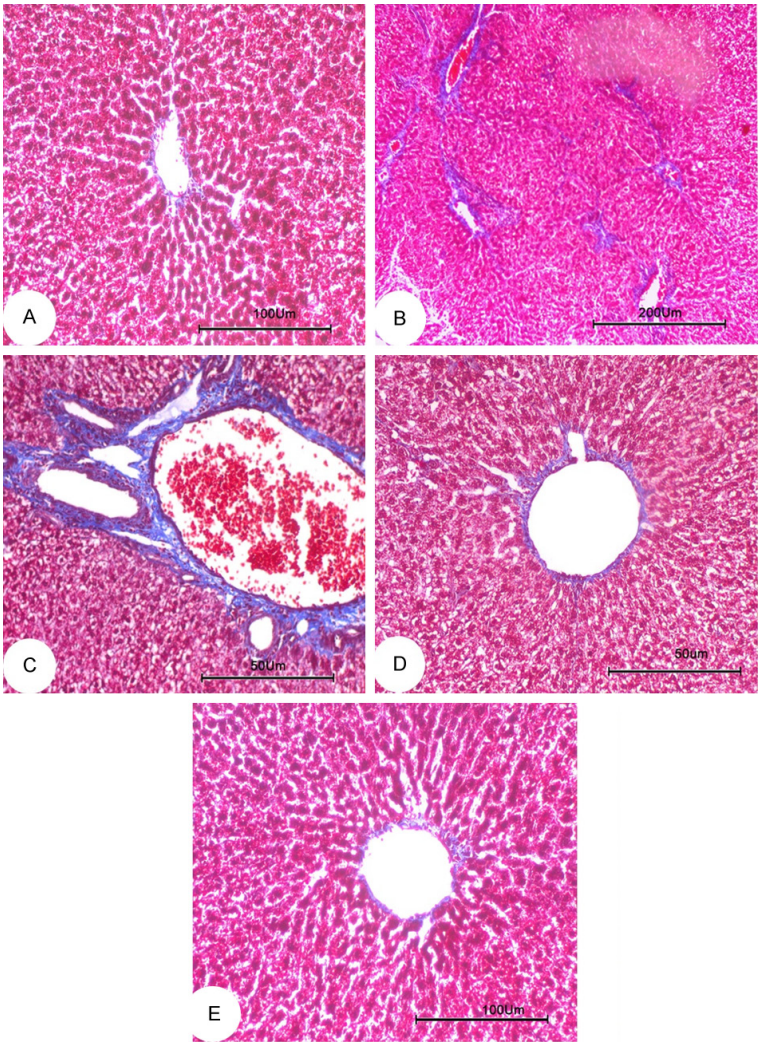

Figure 2. Photomicrographs of liver section of rats. (A) Normal distribution of blue stained fine collagen fibers around the central vein. (B, C) Group CCl4 abundant stained thick collagenous fibers surrounding the portal area and bile duct. (D, E) CCl4/mice and rats' BM-MSCs respectively illustrating marked decrease of collagen fibers (Masson's trichrome stain; Scale bars of A, E = 100 μm, Scale bars of C, D = 50 μm, Scale bars of B = 200 μm).

In contrast to animals treated with CCl4 alone, the liver tissues of animals treated with both CCl4 and BM-MSCs derived from rats (**Figure 1I**) or mice (**Figure 1J**) displayed marked amelioration of the pathological changes of the sinusoids, central vein, and the cytoarchitecture of hepatocytes.

Masson's trichrome staining

Masson's trichrome (MT) highlights collagen fibers in blue stain. In MT-stained liver sections of the control animals, the surroundings of the central vein featured regular distribution of fine collagen fibers (**Figure 2A**). In contrast, sections prepared from the liver of CCl4-treated animals featured an abundance of thick collagenous fibers surrounding the portal area and bile ducts (**Figure 2B**, **2C**). However, the amount of collagen fibers was markedly decreased in animals treated with both CCl4 and BM-MSCs from mice (**Figure 2D**) or rats (**Figure 2E**).

Histopathological change scores of liver lesions

Histopathological change scores of different groups are represented in **Table 4**. The normal control liver section showed no histological lesions as represented by zero score. The liver of CCl4-treated rats displayed different grades of histopathological alterations scores ranging from grade III to grade 0. The treatments of CCl4-administered group with mice BM-MSCs and rats' BM-MSCs revealed marked improvements in histological lesions including steatosis or fatty changes, vacuolar degeneration, vascular congestion, and binuclear hepatocytes, necrosis and collagen fibers as compared with CCl4-treated group.

Immunohistochemical result of liver tissue

TNF-α, p53 and COX-2 expression: The liver levels of TNF-α assayed by immunohistochemistry were summarized in **Figure 3** for animals in the different groups. The pale brown density in the photomicrograph in **Figure 3A** indicated very low levels of TNF-α characteristic of the normal control. In contrast, liver samples from the group treated with CCl4 alone featured intense brown positive immunoreaction for TNF-α in the cytoplasm of hepatocytes (**Figure 3B**). However, hepatocytes of animals treated with both CCl4 and mice or rats' BM-MSCs

Table 4. Histopathological scores of liver lesions in groups of normal control, CCl4, CCl4/mice BM-MSCs, CCl4/rats BM-MSCs

Histopathological changes	Score	Normal Control	CCl4	CCl4/mice BM-MSCs	CCl4/rats BM-MSCs
Steatosis and fatty degeneration	0	6 (100%)	1 (16.7%)	6 (100%)	6 (100%)
	I	-	1 (16.7%)	-	-
	II	-	3 (50%)	-	-
	III	-	1 (16.7)	-	-
Vacuolar degeneration	0	6 (100%)	-	4 (66.7%)	5 (83.3%)
	I	-	1 (16.7%)	1 (16.7%)	1 (16.7%)
	II	-	2 (33.3%)	1 (16.7%)	-
	III	-	3 (50.0%)	-	-
Vascular congestion	0	6 (100%)	-	6 (100%)	6 (100%)
	I	-	-	-	-
	II	-	2 (33.3%)	-	-
	III	-	4 (66.7%)	-	-
Binuclear hepatocytes	0	6 (100%)	1 (16.7%)	5 (83.3%)	5 (83.3%)
	I	-	2 (33.3%)	-	1 (16.7%)
	II	-	3 (50.0%)	1 (16.7%)	-
	III	-	-	-	-
Necrosis	0	6 (100%)	3 (50.0%)	6 (100%)	6 (100%)
	I	-	1 (16.7%)	-	-
	II	-	2 (33.3%)	-	-
	III	-	-	-	-
Collagen fibres	0	6 (100%)	-	4 (66.7%)	4 (66.7%)
	I	-	-	1 (16.7%)	2 (33.3%)
	II	-	2 (33.3%)	1 (16.7%)	-
	III	-	4 (66.7%)	-	-

Histopathological lesions were rated as absence (0), mild (I), moderate (II), and severe (III)

exhibited minimal cytoplasmic positivity for TNF-α (**Figure 3C**, **3D**).

A very similar pattern was observed for the p53 protein levels in liver (**Figure 3**): p53-positive density in the cytoplasm of hepatocytes was pale in the normal control (**Figure 3E**), intense brown in the CCl4-treated (**Figure 3F**), and this pattern was also mirrored by the densities of COX-2 pale again in the CCl4/mice BM-MSCs (**Figure 3G**) and CCl4/rats' BM-MSCs (**Figure 3H**) groups.

This pattern was also mirrored by the densities of COX-2 positive immunoreaction in the cytoplasm of hepatocytes (**Figure 3**). The photomicrograph (**Figure 3I**) illustrated very week expression of COX-2 in normal control group. CCl4-injection revealed strong positive immunoreaction for COX-2 in the cytoplasm of hepatocytes (**Figure 3J**) compared to the control. CCl4/mice BM-MSCs and CCl4/rats' BM-MSCs (**Figure 3K**, **3L**) showed weak immunoreaction for COX-2 in the cytoplasm of hepatocytes.

Results of the quantitative image analysis of the immunohistochemical densities positive for TNF-α, p53, and COX-2 protein, summarized in **Table 5**, confirmed the above qualitative assessments. Specifically, liver levels of these proteins were significantly increased in CCl4-injected rats over those in the normal control but were significantly downregulated in animals receiving both CCl4 injections and treatment with mice or rats' BM-MSCs. The analysis also revealed that the treatment was significantly ($P < 0.05$) more effective with rats' BM-MSCs than with mice BM-MSCs in preventing the CCl4-induced elevations of TNF-α, p53, and COX-2 protein levels in the liver. Alterations in the average area percentage of TNF-α, p53-, and COX-2 immunoreactions in the control,

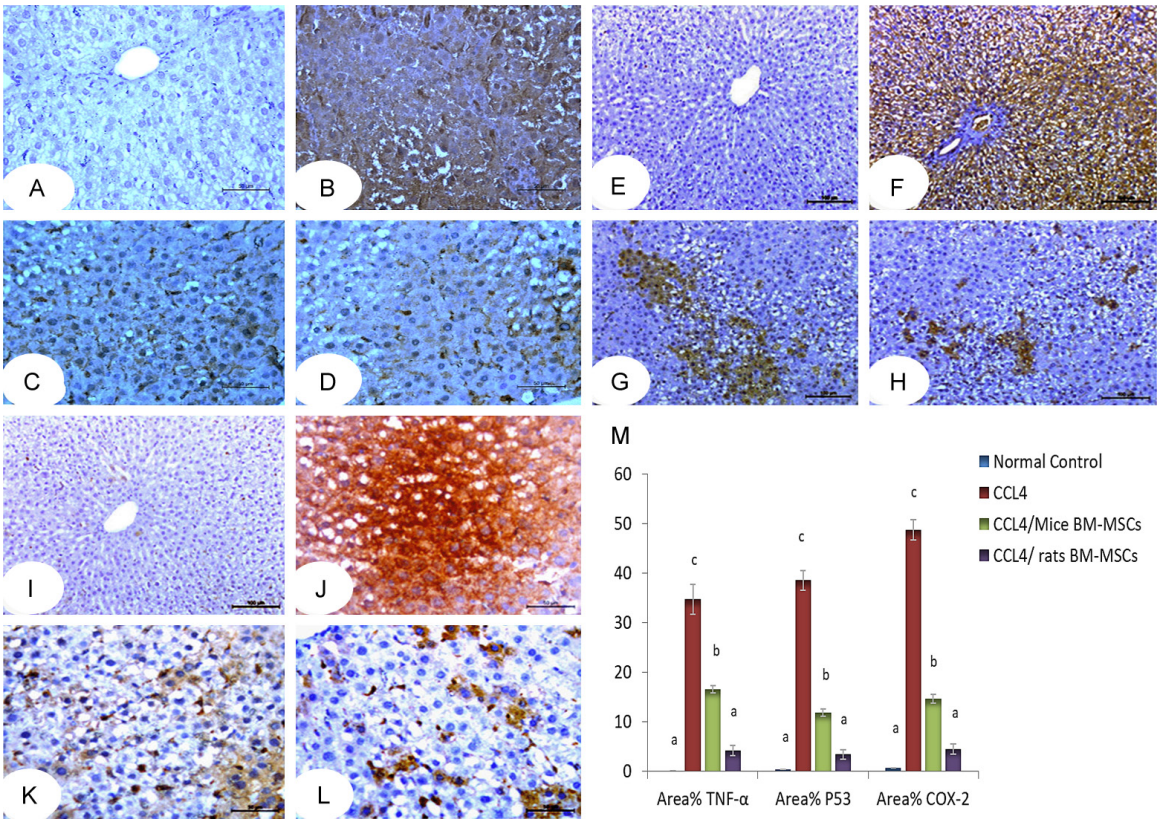

Figure 3. Photomicrographs of liver section. (A) Control group showing negative immunoreaction for TNF-α in the cytoplasm of hepatocytes. (B) CCl4 Group showing intense brown positive immunoreaction for TNF-α in the cytoplasm of hepatocytes. (C) CCl4/mice BM-MSCs and (D) CCl4/rats' BM-MSCs respectively revealing minimal immune reaction for TNF-α in the cytoplasm of hepatocytes (Immunostaning for TNF-α; Scale bars of A-D = 50 μm). (E) Control group showing negative immunoreaction for p53 in the cytoplasm of hepatocytes. (F) CCl4 Group showing intense brown positive immunoreaction for p53 in the cytoplasm of hepatocytes. (G) CCl4/mice BM-MSCs and (H) CCl4/rats' BM-MSCs respectively revealing minimal immune reaction for p53 in the cytoplasm of hepatocytes (Immunostaning for p53; Scale bars of A-D = 100 μm). (I) Control group showing negative reaction for COX-2 in the cytoplasm of hepatocyte. (J) CCl4 Group illustrating strong positive immunoreaction for COX-2 in the cytoplasm of hepatocytes. (K) CCl4/mice BM-MSCs and (L) CCl4/rats' BM-MSCs showing weak immunoreaction for COX-2 in the cytoplasm of hepatocytes (Immunostaning for COX-2; Scale bars of A = 100 μm, Scale bars of B-D = 50 μm). (M) Showing area % of TNF-α, p53 and COX-2 immunohistochemistry in all studied groups. Mean values with different superscript letters are significantly different at $P < 0.05$.

CCl4-injected, and groups given BM-MSCs from rats and mice are shown (**Figure 3M**).

Ultrastructural result of liver tissue

Transmission electron microscopical examination of hepatocytes of the control group showed euchromatic nucleus, nucleolus, numerous mitochondria, rough endoplasmic reticulum, glycogen granules, and bile canaliculi with intact microvilli (**Figure 4A**, **4B**). Normal Kupffer cells (**Figure 4C**) were also observed. In contrast, liver cells in animals of the CCl4-treated group featured shrunk nuclei, variable-size lipid droplets, damaged bile canaliculi, an absence of microvilli, and vacuolated mitochondria (**Figure 4E**, **4F**). In addition, a proliferation of Kupffer cells featuring irregular cell membrane, bundles of collagen fiber, dilatation of bile canaliculi, pyknotic nuclei, and irregular nuclear membrane, was also observed (**Figure 4D**, **4G**).

However, administration of mice BM-MSCs to CCl4-treated animals led to the amelioration of nuclei and mitochondria of hepatocytes and the irregular membrane of Kupffer cells (**Figure 5A**, **5B**). Similarly, administration of rats' BM-MSCs to CCl4-treated animals led to marked recovery of the nucleus, mitochondria, rough endoplasmic reticulum, bile cana-liculi of hepatocytes, and the irregular nuclear membrane of Kupffer cells (**Figure 5C**, **5D**).

Table 5. Showing the changes in the area percentage of TNF-α, p53 and COX-2 immunopositivity in all studied groups

Groups	Area% TNF-α	Area% p53	Area% COX-2
Normal Control	0.04 ± 0.01[a]	0.44 ± 0.02[a]	0.68 ± 0.02[a]
CCl4	34.75 ± 3.01[c]	38.56 ± 1.97[c]	48.78 ± 2.15[c]
CCl4/mice BM-MSCs	16.58 ± 0.70[b]	11.81 ± 0.74[b]	14.62 ± 1.70[b]
CCl4/rats BM-MSCs	4.19 ± 0.70[a]	3.45 ± 0.90[a]	4.48 ± 0.83[a]

Data are represented as mean ± SE. Number of animals in each group is six. Mean values with different superscript letters are significantly different at P < 0.05. a, b, c indicated the difference or similarity between groups.

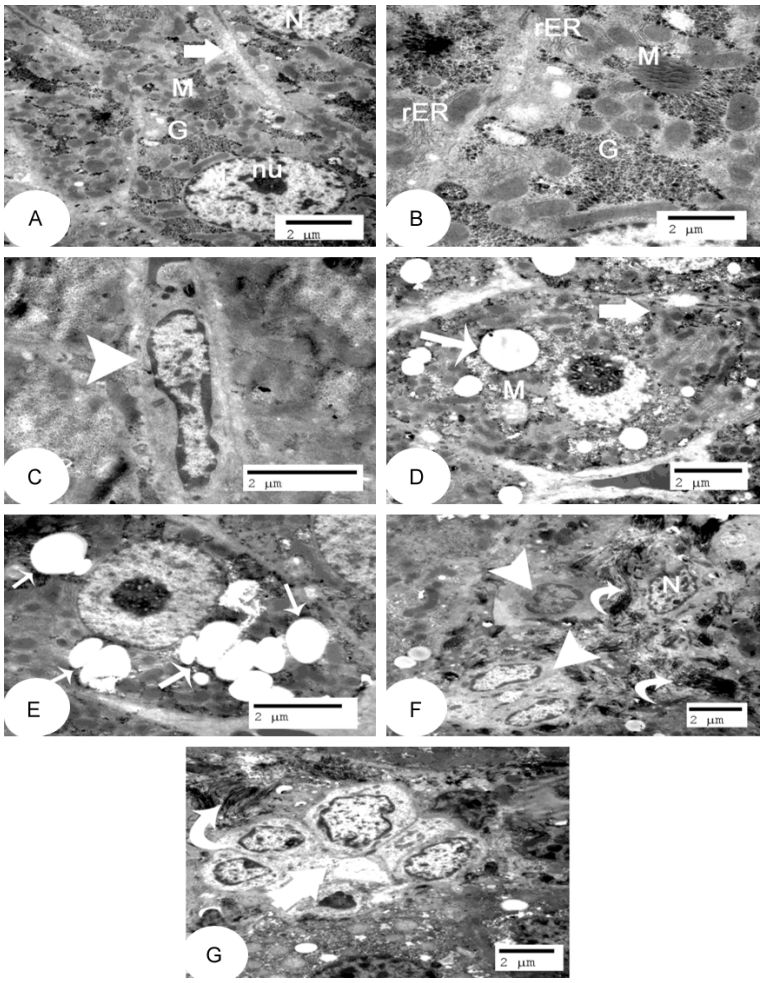

Figure 4. Electron micrographs of liver cells. A, B: Control group showing hepatocytes with euchromatic nucleus (N), nucleolus (nu), numerous mitochondria (M), rough endoplasmic reticulum (rER), glycogen granules (G), and bile canaliculi with intact microvilli (thick arrow) (Scale bar = 2 µm). C: Normal Kupffer cell (head arrow) (Scale bar = 2 µm). D, E: Liver cells of CCl4-treated group showing lipid droplets with variable size droplets (long arrow), damaged bile canaliculi and absence of microvilli (thick arrow), and vacuolated mitochondria (M) (Scale bars = 2 µm). F, G: Liver cells of CCl4 group showing shrinkage nucleus (N), proliferated Kupffer cell with irregular membrane (head arrow), bundle of collagen fiber (curve arrow), dilatation of bile canaliculi with pyknotic nucleus and irregular nuclear membrane (thick arrow) (Scale bars = 2 µm).

Effect of CCl4 and BM-MSCs on gene expression in the liver

TGF-β1, CYP1A1, MMP-9, procollagen-α1, and UGT1A

CCl4 injection caused a significant upregulation of mRNA expression for TGF-β1, CYP1A1, MMP-9, procollagen-α1, and UGT1A (**Figure 6**). Conversely, CCl4 injection caused a downregulation of mRNA expression for IL-4 and IL-10 in the liver (**Figure 7**). But the injection of rats or mice BM-MSCs once a week in CCl4-treated animals restored liver mRNA expression for TGF-β1, CYP1A1, MMP-9, procollagen-α1, and UGT1A to levels similar to those of the control group. However, the increased mRNA expression for IL-4 and IL-10 induced by the BM-MSCs treatment did not fully restore normal levels and was only significant ($P < 0.05$) for IL-10. In comparison to the healthy control group, the CCl4 group had lower levels of CD-105 and Oct3/4 expression (significant P 0.05) (**Figure 8**). On the other hand, the BM-MSCs treatment elevated the mRNA expression of CD-105 and Oct3/4.

Nrf2, caspase-3, TNF-R1, and NF-κB p65

The liver levels of NFE2L2, Caspase-3, TNF-R1, and NF-κB p65 proteins are summarized in **Figure 9**. In the CCl4-injected group, levels of the Nrf2 protein were significantly lower ($P < 0.05$) while levels of caspase-3, TNF-R1, and NF-κB p65 protein were significantly higher ($P < 0.05$) than those in the normal control. The treatment of CCl4-injected rats with mice or rats' BM-MSCs produced a significant increase in

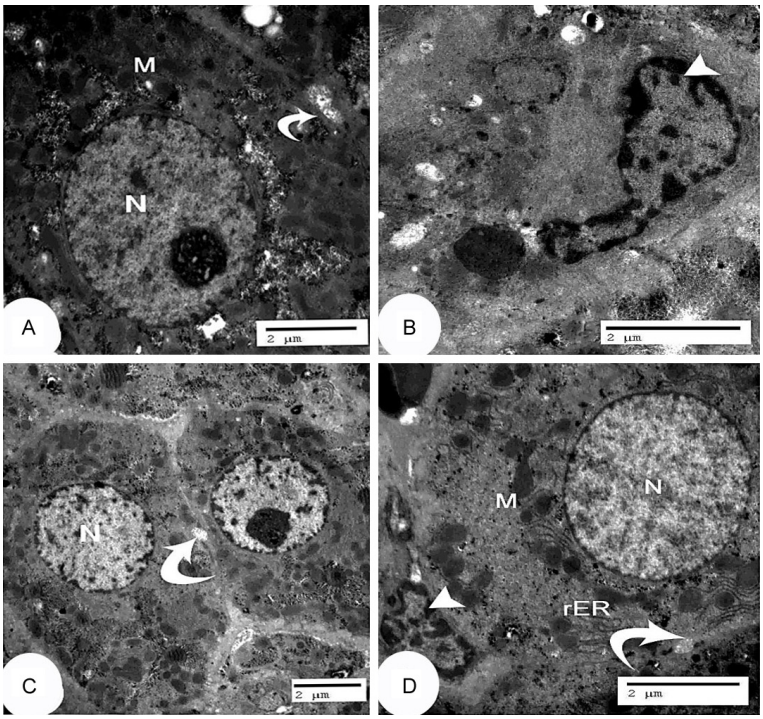

Figure 5. Electron micrographs of hepatocytes. A, B: CCl4/mice BM-MSCs showing amelioration of the hepatocyte nucleus (N) and mitochondria (M) with irregular membrane of Kupffer cell (head arrow). C, D: CCl4-treated groups CCl4/rats' BM-MSCs revealing marked recovery of the hepatocyte nucleus (N), mitochondria (M), rough endoplasmic reticulum (rER), bile canaliculi (carved arrow) and irregular nuclear membrane of Kupffer cell (arrow head) (Scale bars = 2 µm).

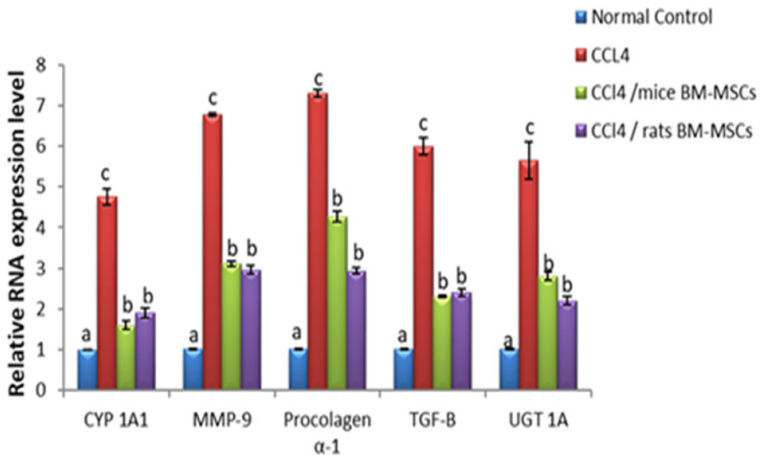

Figure 6. Effect of rats' BM-MSCs and mice BM-MSCs on liver tissue CYP1A1, MMP-9, procollagen-α1, TGF-β1, and UGT1A mRNA expression in CCl4-injected rats. Means that share the same superscript symbol(s) are not significantly different. Number of detected samples in each group is three.

Nrf2 expression, with the rat BM-MSCs being more effective. In contrast, the treatment of CCl4-injected rats with mice or rats' BM-MSCs produced significant downregulation of CCl4-elevated mRNA expression for caspase-3, TNF-R1, and NF-κB p65 protein, with the rats' BM-MSCs being significantly ($P < 0.05$) more effective than the mice BM-MSCs.

Discussion

CCl4-induced liver fibrosis and cirrhosis is a well-known experimental model. Comparatively to mice injected with CCl4/MSCs, animals treated with CCl4 alone exhibited collagen buildup and lipid droplets of varying size. Here, we used this paradigm to examine and contrast the BM-MSC treatment's ameliorative effects on CCl4-induced liver fibrosis and the associated pathological alterations of histological and functional integrity in mice and rats. We also looked into a number of mediators of oxidative stress, inflammation, apoptosis, and fibrosis in an effort to elucidate the processes behind the MSC effect.

We have found that, as a result of hepatocyte injury caused by CCl4 injection, the levels of bilirubin and the activity of blood liver enzymes, such as AST, ALT, ALP, and γ-GT, significantly increased in comparison with those of the normal control group. However, albumin activity significantly decreased below the control in the CCl4-injected group (**Table 2**). These results are in accordance with the findings of Perrissoud [54], El-Haskoury [55], and Barghi [56]. Other investigators also showed that CCl4 toxicity led to an increase in blood liver enzyme activity and total bilirubin level [55, 58].

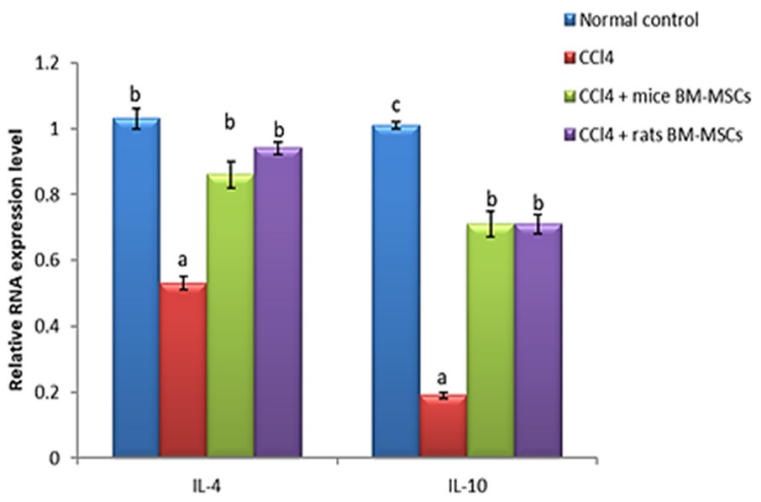

Figure 7. Effect of rats' BM-MSCs and mice BM-MSCs on liver tissue IL-4 and IL-10 mRNA expression in CCl4-injected rats. Means that share the same superscript symbol(s) are not significantly different. Number of detected samples in each group is three.

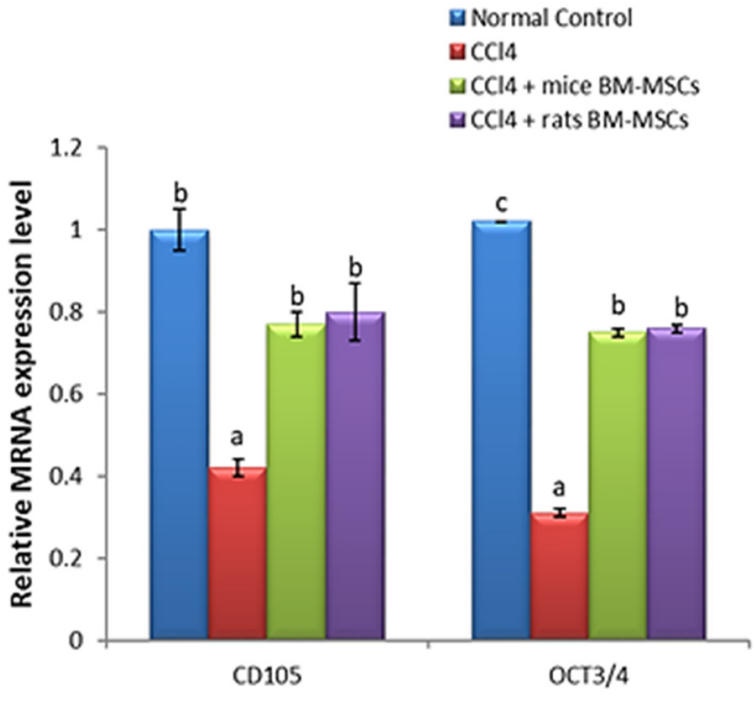

Figure 8. Effect of rats' BM-MSCs and mice BM-MSCs on liver tissue CD105, and Oct3/4 mRNA expressions in CCl4-injected rats. Parameter means that have different symbols are significantly different. Number of detected samples in each group is three.

On the other hand, we have found that treatment of CCl4-injected rats with mice BM-MSCs and rat BM-MSCs improved the CCl4-altered serum ALT, AST, ALP, and γ-GT activities, and albumin and bilirubin levels, toward the normal levels. These findings are consistent with those of Cho [59], Ayatollahi [60], and Zhou [61], who reported similar results for the treatment of CCl4-intoxicated and cirrhotic rats with MSCs.

The advantage of rats' BM-MSCs over mice BM-MSCs was most likely due to the presence of a powerful therapeutic agent for the treatment of liver cirrhosis.

Oxidative stress and excessive production of ROS by chemicals, drugs and toxins result in oxidative damage to DNA, proteins, and lipids. The disorganization, malfunction, and eventual destruction of membranes, enzymes, and proteins are all possible outcomes of this molecular damage [62, 63]. El-Haskoury [54] reported that CCl4 caused an elevation of LPO and a decrease of GPx and GSH in liver cirrhosis, in agreement with our results of CCl4-induced significant increase of liver LPO and decrease of GPx and GST compared to the normal control. Sodhi [64] also reported a decrease of GPx activity levels in the liver due to hepatic damage. A decrease in SOD and GPx activity would most likely lead to a reduction in anti-oxidative capabilities. In this respect, our results are in agreement with those of Khan [65], who reported that CCl4 induced oxidative stress by depleting antioxidants (GSH and GST) and increasing LPO levels in the liver of mice. In contrast, the treatment of CCl4-injected rats with mice and rats' BM-MSCs significantly downregulated the CCl4-elevated liver LPO and significantly countered the CCl4-induced decrease of liver GSH levels and SOD, GST, and GPx activities.

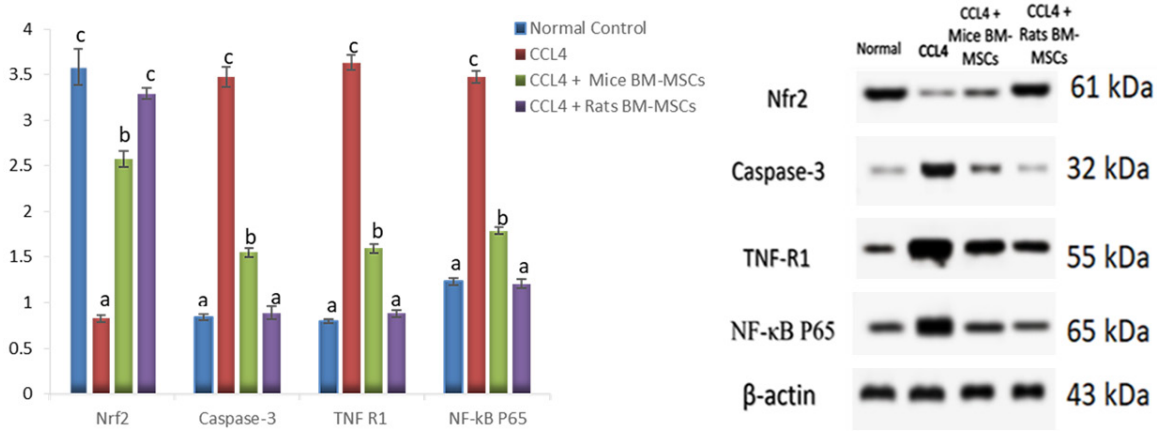

Figure 9. The expression of Nrf2, caspases-3, TNF-R1 and NF-κB P65 in different groups by Western blot analysis. The β-actin was used as the loading control of cleaved Nrf2, caspases-3, TNF-R1 and NF-κB P65. The results of Nrf2, caspases-3, TNF-R1 and NF-κB P65 are presented as relative expression to β-actin (mean ± SE), and a, b, c indicated the difference or similarity between groups.

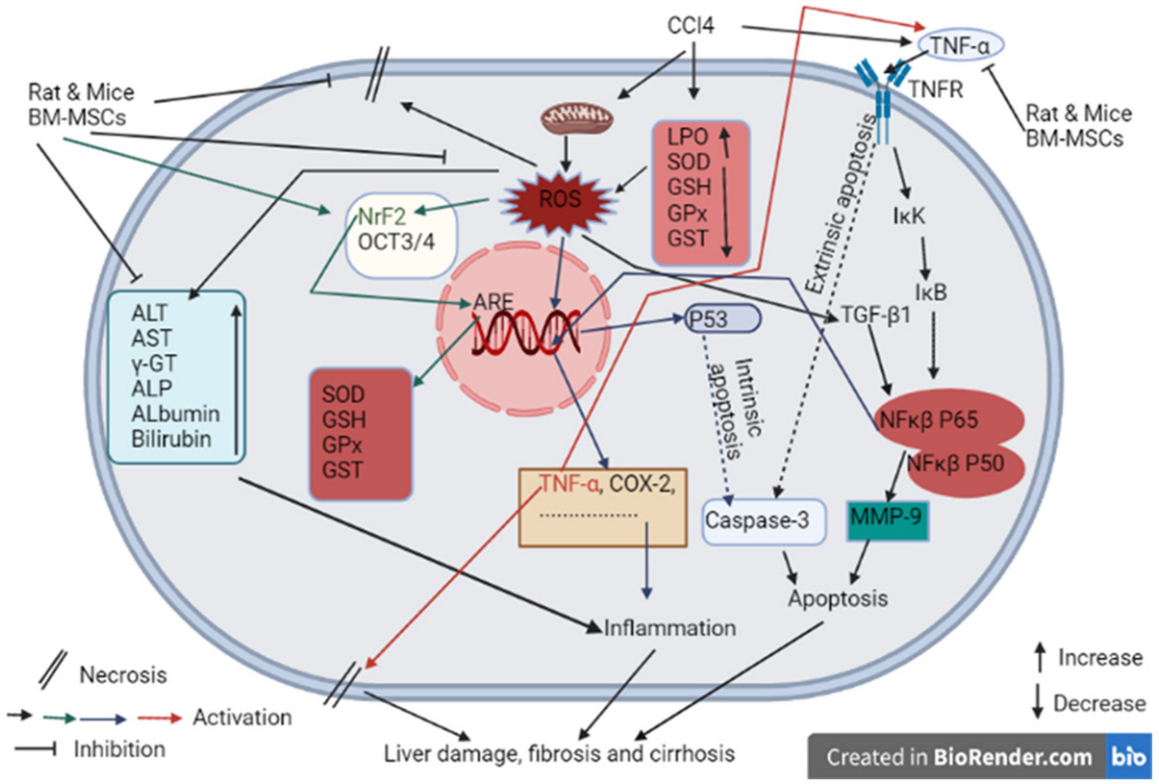

Figure 10. Schematic figure showing the mechanisms of actions of BM-MSCs in preventing CCl4-induced liver injury via suppression of oxidative stress, inflammation and apoptosis.

We also found that rats' BM-MSCs were more potent than mice BM-MSCs. In line with these findings, Ayatollahi [60] observed that MSC-based therapy greatly prevented the CCl4-induced decline of hepatic GSH levels and that GSH levels were significantly higher in MSC-treated mice than in control animals when no CCl4 injections were given. Also, it was shown that MSC transplantation into rat livers that have been injured by iso-chemic/perfusion results in the suppression of oxidative stress and the reduction of apoptosis [66]. The protective

effects exerted by MSCs against CCl4-induced liver hepatotoxicity, which our biochemical analysis revealed, were confirmed by conventional histopathological examination. Specifically, we determined that the histopathological changes observed after the administration of CCl4 were reversed in rats also treated with rats or mice BM-MSCs. These results are in accordance with the findings of Kus [67], Zhang [68], and Magdy [69], who observed marked reduction in the amount of collagen fibers and an overall improvement of the liver tissue in treated animals.

Abdel-Kader [70] and Ahmed [71] reported that CCl4 administration led to the loss of the usual hepatic cytoarchitecture and the appearance of many vacuoles with darkly stained nuclei in most of the liver cells under light microscopic examination. Additionally, the same investigators' electron microscopic analysis of the same tissues revealed that hepatocytes had big irregular vacuoles, many fat droplets, and less than normal mitochondria and rER, which was consistent with our findings. Hepatocyte structural damage brought on by CCl4 was caused by organelle edema [72]. Also consistent with our results, Abdel-Moneim [73] and Lin [74] observed the development of ultrastructural alterations, including the disruption of cisternae, mitochondrial swelling, and lysosomal perturbations, which may reflect the significantly increased hepatic large lipid droplets in CCl4-treated rats. In addition, our electron microscopic observation that hepatocytes of animals treated with MSCs showed marked recovery of the nucleus, mitochondria, rough endoplasmic reticulum, and bile canaliculi of hepatocytes and recovery of normal Kupffer cells are in agreement with those of Ahmed [75] and Abdel-Kader [76]. Similar results, revealing histopathological and ultrastructural improvement in the liver structure of animals treated with CCl4/MSCs relative to animals treated with CCl4 alone, were also reported by Ahmed [71], noting that most of the hepatocytes regained their structural integrity and appeared nearly like those of the normal control.

We found TNF-α at substantially higher levels in CCl4-treated animals than in the normal controls, but treatment with mice and rats' BM-MSCs returned TNF-α immunoreactivity to significantly lower levers. Consistent with our results, Hermenean [77], Domitrović and Jakovac [78] found that TNF-α expression was much higher in the CCl4-treated mice than in the control animals.

The tumor-suppressor protein p53, also known as the proapoptotic protein, controls the transcription of numerous target proteins involved in the cell cycle, differentiation, and apoptosis [79]. A number of proteins strictly control the expression and degradation of p53 in the normal redox state, keeping the level of p53 low [80]. According to Ogaly [81] and Elgawish [82], we discovered that the immunological reactivity for p53 was noticeably elevated in the cytoplasm of hepatocytes in CCl4-treated animals. Nevertheless, these levels were restored upon treatment with mouse and rat BM-MSCs.

Previous studies have demonstrated that COX-2 is upregulated in the cirrhotic liver [83, 84]. Previous studies of liver cirrhosis have demonstrated the involvement of COX-2 in inflammation, activation of hepatic stellate cells, epithelial-mesenchymal transition, and angiogenesis [85-87]. We observed strong positive immunostaining for COX-2 in the cytoplasm of hepatocytes of CCl4-treated animals, consistent with Tang [88] and Hui [89], but weak COX-2 positivity in the control group as well as in CCl4-injected animals treated with mice or rats' BM-MSCs. This ameliorating effect by the rat BM-MSCs was stronger.

In the cirrhotic liver of rats given CCl4 injections, we found that the mRNA expression levels for MMP-9, TGF-1, and procollagen-1 were dramatically elevated above normal levels. However, this was noticeably reduced when the rats' or mice's BM-MSCs were used as a treatment (with rat BM-MSCs being more effective). In line with these findings, Hui [89] showed that CCl4 injection increased MMP-9 mRNA levels, and RT-PCR further demonstrated that procollagen-1 expression was higher in the CCl4 group. Similarly, Chale-Dzul [90] found that CCl4 increased mRNA expression for TGF-β1, and MMP-9, and TGF-β1. Meanwhile, Hsu [91] reported that administration of another hepatotoxin, dimethylnitrosamine (DMN), to rats for 2 and 5 weeks induced progressive increases in hepatic fibrosis scores in association with elevated hepatic mRNA expression for TGF-β1 and procollagen-α1.

Hepatic UGT1A mRNA expression was markedly elevated in CCl4-induced liver cirrhosis; however, expression levels were reduced following administration of BM-MSCs from mice and rats, with the latter being more effective. Consistent with our result, Fei-Yan [92] found that the mRNA levels of hepatic UGT1A were significantly increased above normal in CCl4-treated rats. In a rats' model, rat BM-MSCs functioned better than mice BM-MSCs, probably because rat MSCs are allogeneic (originating from the same species as the host). CYP1A1 mRNA expression in the CCl4-induced liver cirrhosis of rats was higher than normal but decreased in animals also treated with mice or rats' BM-MSCs (the latter was more potent). Our results are consistent with those of Charles and Huang [93], who reported that CYP1A1 mRNA expression in CCl4-treated animals increased above normal levels. CYP1A1 is one of the main cytochrome P450 enzymes (CYPs) and has been examined extensively for its role in the metabolism of drugs and environmental chemicals. The induction of these CYPs contributes to oxidative stress and increased inflammation [94]. On the other hand, therapies with BM-MSCs may result in significant anti-inflammatory and antioxidant effects via downregulating liver CYP1A1 expression (**Figure 10**). Strategic clinical studies will benefit from a better understanding of the heterogeneity and potency of stem cells [95]. Stem cells naturally have the ability to divide indefinitely and, if the conditions are right, to do so without differentiating. So, for correct differentiation, the cells need to receive the right signals from their environment and the cells around them [96]. Modifications in cell-to-cell or cell-environmental signalling may have an impact on the resident cells' functional pathways. Hence, it was found that BM-MSC therapy in rats was more effective than BM-MSC therapy in mice.

In the present study, mRNA expression for CD105 and Oct3/4 in the liver significantly decreased below normal in CCl4-injected rats, but expression levels were significantly increased again upon a treatment of CCl4-injected rats with mice or rat BM-MSCs. Both CD105 and Oct3/4 are specific markers of MSCs [24, 97]. In particular, Oct3/4 is one of the important transcription factors required to maintain the pluripotency and self-renewal of stem cells [42, 98, 99]. In our opinion, the increased levels of CD105 and Oct3/4 in CCl4-injected rats after treatments with BM-MSCs may reflect the homing and multiplication of these cells in the liver.

The mRNA expression for IL-4 and IL-10 significantly decreased below normal in liver of CCl4-injected rats, but this decrease was significantly ameliorated upon treatment with mice or rats' BM-MSCs. IL-4 and IL-10 are both T helper 2 (Th2) cytokines and are known to possess critical anti-inflammatory, immunoregulatory, and protective properties [100-103]. Moreover, IL-10 has been demonstrated to regulate neutrophil infiltration, hepatocyte proliferation, and liver fibrosis in a murine model of CCl4 hepatotoxicity [104, 105], pointing to potential pathways underlying the therapeutic actions of MSCs in the treatment of liver cirrhosis.

Nrf2 is an important transcription factor in the antioxidant response pathway and it is an emerging modulator of cellular resistance to ROS (**Figure 10**). Nrf2 is normally confined to the cytoplasm in normal circumstances. Under oxidative stress, however, Nrf2 reaches the nucleus and works as a transcriptional factor, controlling downstream gene expression and so reducing oxidative stress [106]. It stimulates the basal as well as induced expressions of antioxidant response element (ARE)-dependent genes to control the physiological and pathophysiological outcomes of oxidant exposure [107]. In the current work, rats given CCl4 injections showed a significant drop in the expression of the liver protein Nrf2, and treatment of CCl4-injected rats with either mice or rats' BM-MSCs considerably reduced the downregulation of Nrf2. Rats' BM-MSCs were more successful. There is an accumulating evidence from previous publications that the expression of antioxidant ARE genes, which also exert anti-inflammatory actions, is regulated mainly by the transcription factor Nrf2 [108] (**Figure 9**). In addition, it is worth mentioning that SOD, GPx, and MDA are enzymes that are known to be connected to Nrf2 [109, 110]. Thus, the increase in liver Nrf2 expression may be a key player in mediating the antioxidant and anti-inflammatory effects exerted by BM-MSCs in Wistar rats with CCl4-induced hepatotoxicity (**Figure 9**). The findings demonstrated that treatment with mice and rats' BM-MSCs reduced ROS, oxidative stress, liver enzymes, and inflammation but Nrf2 increased (**Figure 10**).

Consistent with Wang [111], we observed that cleaved caspase-3 expression in the CCl4-injected group was significantly greater than normal. We also saw that BM-MSC therapy brought the levels back to those of normal control, and the impact was stronger when rats' BM-MSCs were used in the treatment rather than mice's. Rat BM-MSC was found by the researchers to reduce CCl4-induced hepatocyte death [112, 113]. BM-MSCs in mice were significantly lower than those in the CCL4 group. Caspase-3 and p53 are mediators in the intrinsic apoptotic pathway that is activated by excessive production in mitochondria (**Figure 10**). This shows that the anti-apoptotic actions of MSCs exerted via the intrinsic route are responsible for the downregulation of these two apoptotic mediators by treatment of CCl4-injected rats with mice's and rats' BM-MSCs (**Figure 10**).

TNF-R1, detected by Western blot in the present study, was significantly reduced after treatment with mice and rats' BM-MSCs compared to the CCl4-injected group. TNF-R1 and other TNF-R transmembrane death receptors, which have a death domain and carry the death signal from the cell surface to the cytoplasmic membrane, are examples of extrinsic transcription factors [114]. The ability of mice and rats' BM-MSCs to treat CCl4-injected rats reflects their capacity to inhibit apoptosis via extrinsic pathway as well, as evidenced by the downregulation of death receptor domain TNF-R1 in these treated rats (**Figure 10**).

Our results indicated that, acting *via* the alteration of NF-κB p65 protein expression, MSCs isolated from the bone marrow of rats or mice may attenuate inflammation in the liver of the CCl4-injected rats. Consistent with our findings, Wang [115] discovered that NF-κB p65 levels were higher in CCl4-injected rates than in the normal control group. Inflammation is brought on by both the p65 and p50 subunits of NF-B activating inflammatory genes to enhance the expression of pro-inflammatory and inflammatory cytokines and chemokines, including TNF-α, COX-2, and others (**Figure 10**). The anti-inflammatory properties and the inhibitory effects of MSCs on the NF-B signalling pathway are reflected in the decrease in NF-κB p65 expression shown in response to the treatment of CCl4-injected rats with BM-MSCs.

Conclusions

This study has shown that rat liver damage caused by CCl4 may be successfully treated with BM-MSCs obtained from mice and rats. The inhibition of oxidative stress, inflammation, and apoptosis, as well as the enhancement of the antioxidant defense system and Nrf2 expression, may all be ways in which BM-MSCs exert their effects. When it came to increasing antioxidant, anti-apoptotic, and anti-inflammatory effects as well as liver function and integrity, BM-MSCs isolated from rats were more effective than those from mice. There are some limitations to the current study regarding signaling pathways of fibrosis, so further research is needed to figure out the molecular mechanisms involved in the formation E-cadherin and collagen I which are implicated in the fibrotic process.

Acknowledgements

The authors extend their appreciation to the Researchers Supporting Project (RSPD2023-R632), King Saud University, Riyadh, Saudi Arabia. The authors also acknowledged Prof. Dr. Dina Sabry, Department of Medical Biochemistry and Molecular Biology, Faculty of Medicine, Cairo University, Cairo, Egypt for performing the Western blot analysis.

Disclosure of conflict of interest

None.

Abbreviations

ALP, Alkaline phosphatase; ALT, Alanine transaminase; ARE, Antioxidant response element; AST, Aspartate transaminase; BM-MSCs, Bone marrow-derived Mesenchymal Stem Cells; CASP-3, Caspase-3; CCl4, Carbon tetrachloride; CD-105, Cluster Differentiation-105; CD-45, Cluster Differentiation-45; cDNA, complementary Deoxyribonucleic Acid; COX-2, Cyclooxygenase-2; CYP1A1, Cytochrome P450 family 1 subfamily A polypeptide 1; CYPs, Cytochrome P450 enzymes; DMN, Dimethylnitrosamine; GPx, Glutathione Peroxidase; GSH, Glutathione; GST, Glutathione Transferase; H&E, Haematoxylin & Eosin; HRP, Horseradish peroxidase; IFN-γ, Interferon gamma; IL-10, Interleukin-10; IL-4, Interleukin-4; LPO, Lipid peroxidation; MDA, Malondialdehyde; MDSCs, Myeloid-derived suppressor cells; MMP-9, Ma-

trix metalloproteinase 9; mRNA, Messenger ribonucleic acid; MSCs, Mesenchymal stem cells; MT, Masson's trichrome; NF-κB p65, Nuclear factor-kappaB p65; Nrf2, Nuclear factor erythroid 2-related factor 2; Oct3/4, Octamer-binding transcription factor 3/4; p53, Protein 53; RNA, Ribonucleic acid; ROS, Reactive oxygen species; SE, standard error; SOD, Superoxide dismutase; SPSS, Statistical Package of Social Sciences; TBST, Tris-buffered saline with Tween 20; TGF-β1, Transforming growth factor-β1; Th2, T helper 2; TNF-R1, Tumor necrosis factor receptor 1; TNF-α, Tumor necrosis factor-α; UGT1A, Uridine diphospahteglucuronosyl transferase 1A; γ-GT, Gamma-glutamyl transferase.

Address correspondence to: Manal Abdul-Hamid, Division of Histology and Cell Biology, Department of Zoology, Faculty of Science, Beni-Suef University, Salah Salem St., Beni-Suef 62511, Egypt. Tel: +20-082-2334551; ORCID: 0000-0002-0877-3097; Fax: +20-082-2334551; E-mail: medo_bio@yahoo.com; manal.mohamed3@science.bsu.edu.eg; Taghreed N Almanaa, Department of Botany and Microbiology, College of Science, King Saud University, Riyadh 11451, Saudi Arabia. E-mail: talmanaa@ksu.edu.sa

References

[1] Mohamed NZ, Abd-Alla HI, Aly HF, Mantawy M, Ibrahim N and Hassan SA. CCl4-induced hepatonephrotoxicity: protective effect of nutraceuticals on inflammatory factors and antioxidative status in rat. J Appl Pharm Sci 2014; 4: 87-100.

[2] Xu JY, Su YY, Cheng JS, Li SX, Liu R, Li WX and Li QN. Protective effects of fullerenol on carbon tetrachloride-induced acute hepatotoxicity and nephrotoxicity in rats. Carbon 2010; 48: 1388-1396.

[3] Mohammed NR, Ahmed RH, Roshdy NK, Aref MI, Hassan NM and Saleh HE. Effect of bone marrow-derived mesenchymal stem cells and umbilical cord blood-CD34+ cells on experimental rat liver fibrosis. Int J Stem Cell Res Transplant 2014; 2: 63-68.

[4] Di Paola R, Modafferi S, Siracusa R, Cordaro M, D'Amico R, Ontario ML, Interdonato L, Salinaro AT, Fusco R, Impellizzeri D, Calabrese V and Cuzzocrea S. S-acetyl-glutathione attenuates carbon tetrachloride-induced liver injury by modulating oxidative imbalance and inflammation. Int J Mol Sci 2022; 23: 4429.

[5] Khan RA, Khan MR and Sahreen S. CCl4-induced hepatotoxicity: protective effect of rutin on p53, CYP2E1 and the antioxidative status in rat. BMC Complement Altern Med 2012; 12: 178.

[6] Friedman SL. Molecular regulation of hepatic fibrosis, an integrated cellular response to tissue injury. J Biol Chem 2000; 275: 2247-2250.

[7] Nwaechefu OO, Olaolu TD, Akinwunmi IR, Ojezele OO and Olorunsogo OO. Cajanus cajan ameliorated CCl4-induced oxidative stress in Wistar rats via the combined mechanisms of anti-inflammation and mitochondrial-membrane transition pore inhibition. J Ethnopharmacol 2022; 289: 114920.

[8] Wang M, Niu J, Ou L, Deng B, Wang Y and Li S. Zerumbone protects against carbon tetrachloride (CCl4)-induced acute liver injury in mice via inhibiting oxidative stress and the inflammatory response: involving the TLR4/NF-κB/COX-2 pathway. Molecules 2019; 24: 1964.

[9] El-Missiry MA, ElKomy MA, Othman AI and AbouEl-Ezz AM. Punicalagin ameliorates the elevation of plasma homocysteine, amyloid-β, TNF-α and apoptosis by advocating antioxidants and modulating apoptotic mediator proteins in brain. Biomed Pharmacother 2018; 102: 472-480.

[10] Chen S, Akbar SM, Abe M, Hiasa Y and Onji M. Immunosuppressive functions of hepatic myeloid-derived suppressor cells of normal mice and in a murine model of chronic hepatitis B virus. Clin Exp Immunol 2011; 166: 134-142.

[11] Pallett LJ, Gill US, Quaglia A, Sinclair LV, Jover-Cobos M, Schurich A, Singh KP, Thomas N, Das A, Chen A, Fusai G, Bertoletti A, Cantrell DA, Kennedy PT, Davies NA, Haniffa M and Maini MK. Metabolic regulation of hepatitis B immunopathology by myeloid-derived suppressor cells. Nat Med 2015; 21: 591-600.

[12] Gabrilovich DI and Nagaraj S. Myeloid-derived suppressor cells as regulators of the immune system. Nat Rev Immunol 2009; 9: 162-174.

[13] Gregory SH, Sagnimeni AJ and Wing EJ. Bacteria in the bloodstream are trapped in the liver and killed by immigrating neutrophils. J Immunol 1996; 157: 2514-2520.

[14] Golden-Mason L, Kelly AM, Doherty DG, Traynor O, McEntee G, Kelly J, Hegarty JE and O'Farrelly C. Hepatic interleuklin 15 (IL-15) expression: implications for local NK/NKT cell homeostasis and development. Clin Exp Immunol 2004; 138: 94-101.

[15] Kelly AM, Golden-Mason L, Traynor O, Geoghegan J, McEntee G, Hegarty JE and O'Farrelly C. Changes in hepatic immunoregulatory cytokines in patients with metastatic colorectal carcinoma: implications for hepatic anti-tumour immunity. Cytokine 2006; 35: 171-179.

[16] Schwartz RE, Reyes M, Koodie L, Jiang Y, Blackstad M, Lund T, Lenvik T, Johnson S, Hu

WS and Verfaillie CM. Multipotent adult progenitor cells from bone marrow differentiate into functional hepatocyte-like cells. J Clin Invest 2002; 109: 1291-1302.
[17] Lee KD, Kuo TK, Whang-Peng J, Chung YF, Lin CT, Chou SH, Chen JR, Chen YP and Lee OK. In vitro hepatic differentiation of human mesenchymal stem cells. Hepatology 2004; 40: 1275-1284.
[18] Mangi AA, Noiseux N, Kong D, He H, Rezvani M, Ingwall JS and Dzau VJ. Mesenchymal stem cells modified with Akt prevent remodeling and restore performance of infarcted hearts. Nat Med 2003; 9: 1195-1201.
[19] Ortiz LA, Gambelli F, McBride C, Gaupp D, Baddoo M, Kaminski N and Phinney DG. Mesenchymal stem cell engraftment in lung is enhanced in response to bleomycin exposure and ameliorates its fibrotic effects. Proc Natl Acad Sci U S A 2003; 100: 8407-8411.
[20] Fang B, Shi M, Liao L, Yang S, Liu Y and Zhao RC. Systemic infusion of FLK1+ mesenchymal stem cells ameliorate carbon tetrachloride-induced liver fibrosis in mice. Transplantation 2004; 78: 83-88.
[21] Rockel JS, Rabani R and Viswanathan S. Antifibrotic mechanisms of exogenously-expanded mesenchymal stromal cells for fibrotic diseases. Semin Cell Dev Biol 2020; 101: 87-103.
[22] Sakaida I, Terai S, Yamamoto N, Aoyama K, Ishikawa T, Nishina H and Okita K. Transplantation of bone marrow cells reduces CCl4-induced liver fibrosis in mice. Hepatology 2004; 40: 1304-1311.
[23] Wali AF, Ali S, Rashid S, Alsaffar RM, Arafah A, Qamar W and Rehman MU. Attenuation of oxidative damage-associated hepatotoxicity by piperine in CCl4-induced liver fibrosis. J King Saud Univ Sci 2021; 33: 101629.
[24] Chaudhary JK and Rath PC. A simple method for isolation, propagation, characterization and differentiation of adult mouse bone marrow-derived multipotent mesenchymal stem cells. J Cell Sci Ther 2017; 8: 1-10.
[25] Ahmed OM, Hassan MA and Saleh AS. Combinatory effect of hesperetin and mesenchymal stem cells on the deteriorated lipid profile, heart and kidney functions and antioxidant activity in STZ-induced diabetic rats. Biocell 2020; 44: 27-39.
[26] Abd-Allah GA, El-Bakry KA, Bahnasawy MH and El-Khodary ER. Protective effects of curcumin and ginger on liver cirrhosis induced by carbon tetrachloride in rats. Int J Pharmacol 2016; 12: 361-369.
[27] Mohamed TA, Abouel-Nour MF, Eldemerdash RS and Elgalady DA. Therapeutic effects of bone marrow stem cells in diabetic rats. J Comput Sci Syst Biol 2016; 9: 058-068.
[28] Schumann G and Klauke R. New IFCC reference procedures for the determination of catalytic activity concentrations of five enzymes in serum: preliminary upper reference limits obtained in hospitalized subjects. Clin Chim Acta 2003; 327: 69-79.
[29] Tietz NW. Text book of clinical chemistry. In: Burtis CA, Ashwood ER. WB Saunders; 1999. pp. 1431.
[30] Tietz NW. Method of the estimation of lipoprotein concentration without ultracentrifugation. Tietz Fundamentals of Clinical Chemistry. 2nd edition. Philadelphia: WB Saunders company; 1976.
[31] Jendrassik L and Grof P. Quantitative determination of total and direct bilirubin in serum and plasma. Biochem Z 1938; 297: 81-9.
[32] Gendler S. Uric acid. In: Kaplan A, editors. Clin Chem The CV Mosby Co. St Louis, Toronto: Princeton; 1984. pp. 1268-73.
[33] Yagi K. Lipid peroxides and human diseases. Chem Phys Lipids 1987; 45: 337-351.
[34] Marklund S and Marklund G. Involvement of the superoxide anion radical in the autoxidation of pyrogallol and a convenient assay for superoxide dismutase. Eur J Biochem 1974; 47: 469-74.
[35] Beutler E, Duron O and Kelly BM. Improved method for the determination of blood glutathione. J Lab Clin Med 1963; 61: 882-888.
[36] Matkovics B, Kotorman M, Varga IS, Hai DQ and Varga C. Oxidative stress in experimental diabetes induced by streptozotocin. Acta Physiol Hung 1997-1998; 85: 29-38.
[37] Mannervik B and Guthenberg C. Glutathione transferase (human placenta). Methods Enzymol 1981; 77: 231-235.
[38] Shalaby YM, Menze ET, Azab SS and Awad AS. Involvement of Nrf2/HO-1 antioxidant signaling and NF-κB inflammatory response in the potential protective effects of vincamine against methotrexate-induced nephrotoxicity in rats: cross talk between nephrotoxicity and neurotoxicity. Arch Toxicol 2019; 93: 1417-31.
[39] Diah S, Zhang GX, Nagai Y, Zhang W, Gang L, Kimura S, Hamid MR, Tamiya T, Nishiyama A and Hitomi H. Aldosterone induces myofibroblastic transdifferentiation and collagen gene expression through the Rho-kinase dependent signaling pathway in rat mesangial cells. Exp Cell Res 2008; 314: 3654-62.
[40] Zhang YM, Chen XM, Wu D, Shi SZ, Yin Z, Ding R and Lü Y. Expression of tissue inhibitor of matrix metalloproteinases-1 during aging in rat liver. World J Gastroenterol 2005; 11: 3696-700.
[41] Matsuda S, Uchikawa R, Yamada M and Arizono N. Cytokine mRNA expression profiles in

rats infected with the intestinal nematode Nippostrongylus brasiliensis. Infect Immun 1995; 63: 4653-60.
[42] Guo X, Tang Y, Zhang P, Li S, Chen Y, Qian B, Shen H and Zhao N. Effect of ectopic high expression of transcription factor OCT4 on the "stemness" characteristics of human bone marrow-derived mesenchymal stromal cells. Stem Cell Res Ther 2019; 10: 160.
[43] Nakamura T, Torimura T, Sakamoto M, Hashimoto O, Taniguchi E, Inoue K, Sakata R, Kumashiro R, Murohara T, Ueno T and Sata M. Significance and therapeutic potential of endothelial progenitor cell transplantation in a cirrhotic liver rat model. Gastroenterology 2007; 133: 91-107, e1.
[44] Katsanou ES, Kyriakopoulou K, Emmanouil C, Fokialakis N, Skaltsounis AL and Machera K. Modulation of CYP1A1 and CYP1A2 hepatic enzymes after oral administration of Chios mastic gum to male Wistar rats. PLoS One 2014; 9: e100190.
[45] Zhu C, Zhai X, Chen F, Wang N, Zhang X and Lu Y. Capsaicin induces metabolism of simvasatin in rat: involvement of upregulating expression of Ugt1a1. Pharmazie 2016; 71: 269-73.
[46] Kumar K, Das K, Madhusoodan AP, Kumar A, Singh P, Mondal T and Bag S. Rat bone marrow derived mesenchymal stem cells differentiate to germ cell like cells. bioRxiv 2018; 1: 418962.
[47] Bancroft J and Gamble M. Throry and Practice of Histological Techniques. 5th edition. Edinburg: Churchill Livingstone Pup; 2002. pp. 172-175.
[48] Suvarna SK, Layton C and Bancroft JD. Bancroft's theory and practice of histological techniques. 7th edition. Pbl. London: Churchill Livingstone, Elsiver; 2013. pp. 173-87.
[49] Arsad SS, Esa NM and Hamzah H. Histopathologic changes in liver and kidney tissues from male Sprague Dawley rats treated with Rhaphidophora decursiva (Roxb.) Schott extract. J Cytol Histol 2014; S4: 1-6.
[50] Cemek M, Kağa S, Şimşek N, Büyükokuroğlu ME and Konuk M. Antihyperglycemic and antioxidative potential of Matricaria chamomilla L. in streptozotocin-induced diabetic rats. J Nat Med 2008; 62: 284-93.
[51] Bozzola JJ and Russell LD. Electron microscopy: principles and techniques for biologists. Jones & Bartlett Learning; 1999.
[52] Duncan BD. Multiple ranges tests for correlated and heteroscedastic means. Biometrics 1957; 13: 359-364.
[53] Aslan A, Gok O, Erman O and Kuloglu T. Ellagic acid impedes carbontetrachloride-induced liver damage in rats through suppression of NF-kB, Bcl-2 and regulating Nrf-2 and caspase pathway. Biomed Pharmacother 2018; 105: 662-669.
[54] Perrissoud D, Auderset G, Reymond O and Maignan MF. The effect of carbon tetrachloride on isolated rat hepatocytes. Virchows Arch B Cell Pathol Incl Mol Pathol 1981; 35: 83-91.
[55] El-Haskoury R, Al-Waili N, Kamoun Z, Makni M, Al-Waili H and Lyoussi B. Antioxidant activity and protective effect of carob honey in CCl4-induced kidney and liver injury. Arch Med Res 2018; 49: 306-313.
[56] Barghi M, Ashrafi M, Aminlari M, Namazi F and Nazifi S. The protective effect of Zataria multiflora Boiss essential oil on CCl4 induced liver fibrosis in rats. Drug Chem Toxicol 2021; 44: 229-237.
[57] Mistry S, Dutt KR and Jena J. Protective effect of Sida cordata leaf extract against CCl4 induced acute liver toxicity in rats. Asian Pac J Trop Med 2013; 6: 280-4.
[58] Ponmari G, Annamalai A, Gopalakrishnan VK, Lakshmi PT and Guruvayoorappan C. NF-κB activation and proinflammatory cytokines mediated protective effect of Indigofera caerulea Roxb. on CCl4 induced liver damage in rats. Int Immunopharmacol 2014; 23: 672-80.
[59] Cho KA, Woo SY, Seoh JY, Han HS and Ryu KH. Mesenchymal stem cells restore CCl4-induced liver injury by an antioxidative process. Cell Biol Int 2012; 36: 1267-74.
[60] Ayatollahi M, Hesami Z, Jamshidzadeh A and Gramizadeh B. Antioxidant effects of bone marrow mesenchymal stem cell against carbon tetrachloride-induced oxidative damage in rat livers. Int J Organ Transplant Med 2014; 5: 166-73.
[61] Zhou X, Yang J, Liu Y, Li Z, Yu J, Wei W, Chen Q, Li C and Tang N. Observation of the effect of bone marrow mesenchymal stem cell transplantation by different interventions on cirrhotic rats. Braz J Med Biol Res 2019; 52: e7879.
[62] Slater TF and Sawyer BC. The stimulatory effects of carbon tetrachloride on peroxidative reactions in rat liver fractions in vitro. Inhibitory effects of free-radical scavengers and other agents. Biochem J 1971; 123: 823-828.
[63] Kazek M, Kaczmarek A, Wrońska AK and Boguś MI. Conidiobolus coronatus induces oxidative stress and autophagy response in Galleria mellonella larvae. PLoS One 2020; 15: e0228407.
[64] Sodhi CP, Rana S, Mehta S, Vaiphei K, Goel RC and Mehta SK. Study of oxidative-stress in rifampicin-induced hepatic injury in growing rats with and without protein-energy malnutrition. Hum Exp Toxicol 1997; 16: 315-321.
[65] Khan A, Shal B, Naveed M, Shah FA, Atiq A, Khan NU, Kim YS and Khan S. Matrine amelio-

rates anxiety and depression-like behaviour by targeting hyperammonemia-induced neuroinflammation and oxidative stress in CCl4 model of liver injury. Neurotoxicology 2019; 72: 38-50.
[66] Jin G, Qiu G, Wu D, Hu Y, Qiao P, Fan C and Gao F. Allogeneic bone marrow-derived mesenchymal stem cells attenuate hepatic ischemia-reperfusion injury by suppressing oxidative stress and inhibiting apoptosis in rats. Int J Mol Med 2013; 31: 1395-1401.
[67] Kus I, Ogeturk M, Oner H, Sahin S, Yekeler H and Sarsilmaz M. Protective effects of melatonin against carbon tetrachloride-induced hepatotoxicity in rats: a light microscopic and biochemical study. Cell Biochem Funct 2005; 23: 169-74.
[68] Zhang Y, Jia Y, Yang M, Yang P, Tian Y, Xiao A and Wen A. The impaired disposition of probe drugs is due to both liver and kidney dysfunctions in CCl4-model rats. Environ Toxicol Pharmacol 2012; 33: 453-8.
[69] Magdy BW, Mohamed FE, Amin AS and Rana SS. Ameliorative effect of antioxidants (vitamins C and E) against abamectin toxicity in liver, kidney and testis of male albino rats. J Basic Applied Zool 2016; 77: 69-82.
[70] Abdel-Kader MS, Abulhamd AT, Hamad AM, Alanazi AH, Ali R and Alqasoumi SI. Evaluation of the hepatoprotective effect of combination between hinokiflavone and Glycyrrhizin against CCl4 induced toxicity in rats. Saudi Pharm J 2018; 26: 496-503.
[71] Ahmed SK, Mohammed SA, Khalaf G and Fikry H. Role of bone marrow mesenchymal stem cells in the treatment of CCL4 induced liver fibrosis in albino rats: a histological and immunohistochemical study. Int J Stem Cells 2014; 7: 87-97.
[72] Tasci I, Mas N, Mas MR, Tuncer M and Comert B. Ultrastructural changes in hepatocytes after taurine treatment in CCl4 induced liver injury. World J Gastroenterol 2008; 14: 4897-902.
[73] Abdel-Moneim AM, Al-Kahtani MA, El-Kersh MA and Al-Omair MA. Free radical-scavenging, anti-inflammatory/anti-fibrotic and hepatoprotective actions of taurine and silymarin against CCl4 induced rat liver damage. PLoS One 2015; 10: e0144509.
[74] Lin SY, Dan X, Du XX, Ran CL, Lu X, Ren SJ, Tang ZT, Yin LZ, He CL, Yuan ZX, Fu HL, Zhao XL and Shu G. Protective effects of salidroside against carbon tetrachloride (CCl4)-induced liver injury by initiating mitochondria to resist oxidative stress in mice. Int J Mol Sci 2019; 20: 3187.
[75] Ahmed AF, Mahmoud MF, Ouf MA and El-Fathaah EA. Aminoguanidine potentiates the hepatoprotective effect of silymarin in CCL4 treated rats. Ann Hepatol 2011; 10: 207-15.
[76] Abdel-Kader MS, Soliman GA, Alqarni MH, Hamad AM, Foudah AI and Alqasoumi SI. Chemical composition and protective effect of Juniperus sabina L. essential oil against CCl4 induced hepatotoxicity. Saudi Pharm J 2019; 27: 945-51.
[77] Hermenean A, Mariasiu T, Navarro-González I, Vegara-Meseguer J, Miutescu E, Chakraborty S and Pérez-Sánchez H. Hepatoprotective activity of chrysin is mediated through TNF-α in chemically-induced acute liver damage: an in vivo study and molecular modeling. Exp Ther Med 2017; 13: 1671-80.
[78] Domitrović R and Jakovac H. Effects of standardized bilberry fruit extract (Mirtoselect®) on resolution of CCl4-induced liver fibrosis in mice. Food Chem Toxicol 2011; 49: 848-54.
[79] Vousden KH and Prives C. Blinded by the light: the growing complexity of p53. Cell 2009; 137: 413-31.
[80] Kruse JP and Gu W. Modes of p53 regulation. Cell 2009; 137: 609-22.
[81] Ogaly HA, Eltablawy NA and Abd-Elsalam RM. Antifibrogenic influence of Mentha piperita L. essential oil against CCl4-induced liver fibrosis in rats. Oxid Med Cell Longev 2018; 2018: 4039753.
[82] Elgawish RAR, Rahman HGA and Abdelrazek HMA. Green tea extract attenuates CCl4-induced hepatic injury in male hamsters via inhibition of lipid peroxidation and p53-mediated apoptosis. Toxicol Rep 2015; 2: 1149-56.
[83] Mohammed NA, Abd El-Aleem SA, El-Hafiz HA and McMahon RF. Distribution of constitutive (COX-1) and inducible (COX-2) cyclooxygenase in postviral human liver cirrhosis: a possible role for COX-2 in the pathogenesis of liver cirrhosis. J Clin Pathol 2004; 57: 350-4.
[84] Giannitrapani L, Ingrao S, Soresi M, Florena AM, La Spada E, Sandonato L, D'Alessandro N, Cervello M and Montalto G. Cyclooxygenase-2 expression in chronic liver diseases and hepatocellular carcinoma: an immunohistochemical study. Ann N Y Acad Sci 2009; 1155: 293-9.
[85] Zhao Y, Wang Y, Wang Q, Liu Z, Liu Q and Deng X. Hepatic stellate cells produce vascular endothelial growth factor via phospho-p44/42 mitogen-activated protein kinase/cyclooxygenase-2 pathway. Mol Cell Biochem 2012; 359: 217-23.
[86] Wen SL, Gao JH, Yang WJ, Lu YY, Tong H, Huang ZY, Liu ZX and Tang CW. Celecoxib attenuates hepatic cirrhosis through inhibition of epithelial-to-mesenchymal transition of hepatocytes. J Gastroenterol Hepatol 2014; 29: 1932-42.

[87] Sacerdoti D, Pesce P, Di Pascoli M, Brocco S, Cecchetto L and Bolognesi M. Arachidonic acid metabolites and endothelial dysfunction of portal hypertension. Prostaglandins Other Lipid Mediat 2015; 120: 80-90.
[88] Tang SH, Gao JH, Wen SL, Tong H, Yan ZP, Liu R and Tang CW. Expression of cyclooxygenase-2 is correlated with lncRNA-COX-2 in cirrhotic mice induced by carbon tetrachloride. Mol Med Rep 2017; 15: 1507-1512.
[89] Hui AY, Leung WK, Chan HL, Chan FK, Go MY, Chan KK, Tang BD, Chu ES and Sung JJ. Effect of celecoxib on experimental liver fibrosis in rat. Liver Int 2006; 26: 125-36.
[90] Chale-Dzul J, Pérez-Cabeza de Vaca R, Quintal-Novelo C, Olivera-Castillo L and Moo-Puc R. Hepatoprotective effect of a fucoidan extract from Sargassum fluitans Borgesen against CCl4-induced toxicity in rats. Int J Biol Macromol 2020; 145: 500-509.
[91] Hsu YC, Chiu YT, Lee CY, Lin YL and Huang YT. Increases in fibrosis-related gene transcripts in livers of dimethylnitrosamine-intoxicated rats. J Biomed Sci 2004; 11: 408-17.
[92] Li FY, Xie H, Weng L, Wang H, Cao LJ, Hao HP and Wang GJ. Effects of diammonium glycyrrhizinate on hepatic and intestinal UDP-Glucuronosyltransferases in rats: implication in herb-drug interactions. Chin J Nat Med 2016; 14: 534-40.
[93] Charles AL and Huang TC. Sweet cassava polysaccharide extracts protects against CCl4 liver injury in Wistar rats. Food Hydrocolloids 2009; 23: 1494-500.
[94] Hussain T, Al-Attas OS, Al-Daghri NM, Mohammed AA, De Rosas E, Ibrahim S, Vinodson B, Ansari MG and El-Din KI. Induction of CYP1A1, CYP1A2, CYP1B1, increased oxidative stress and inflammation in the lung and liver tissues of rats exposed to incense smoke. Mol Cell Biochem 2014; 391: 127-36.
[95] Kuchina A, Espinar L, Garcia-Ojalvo J and Süel GM. Reversible and noisy progression towards a commitment point enables adaptable and reliable cellular decision-making. PLoS Comput Biol 2011; 7: e1002273.
[96] Cahan P and Daley GQ. Origins and implications of pluripotent stem cell variability and heterogeneity. Nat Rev Mol Cell Biol 2013; 14: 357-68.
[97] Huang S, Xu L, Sun Y, Wu T, Wang K and Li G. An improved protocol for isolation and culture of mesenchymal stem cells from mouse bone marrow. J Orthop Translat 2014; 3: 26-33.
[98] Takahashi K and Yamanaka S. Induction of pluripotent stem cells from mouse embryonic and adult fibroblast cultures by defined factors. Cell 2006; 126: 663-676.
[99] Okada M, Oka M and Yoneda Y. Effective culture conditions for the induction of pluripotent stem cells. Biochim Biophys Acta 2010; 1800: 956-63.
[100] Bogdan C, Vodovotz Y and Nathan C. Macrophage deactivation by interleukin 10. J Exp Med 1991; 174: 1549-55.
[101] Stordeur P and Goldman M. Interleukin-10 as a regulatory cytokine induced by cellular stress: molecular aspects. Int Rev Immunol 1998; 16: 501-22.
[102] Koulis A and Robinson DS. The anti-inflammatory effects of interleukin-10 in allergic disease. Clin Exp Allergy 2000; 30: 747-50.
[103] Moore KW, de Waal Malefyt R, Coffman RL and O'Garra A. Interleukin-10 and the interleukin-10 receptor. Annu Rev Immunol 2001; 19: 683-765.
[104] Louis H, Van Laethem JL, Wu W, Quertinmont E, Degraef C, Van den Berg K, Demols A, Goldman M, Le Moine O, Geerts A and Devière J. Interleukin-10 controls neutrophilic infiltration, hepatocyte proliferation, and liver fibrosis induced by carbon tetrachloride in mice. Hepatology 1998; 28: 1607-1615.
[105] Thompson K, Maltby J, Fallowfield J, McAulay M, Millward-Sadler H and Sheron N. Interleukin-10 expression and function in experimental murine liver inflammation and fibrosis. Hepatology 1998; 28: 1597-606.
[106] Ni YH, Huo LJ and Li TT. Antioxidant axis Nrf2-keap1-ARE in inhibition of alcoholic liver fibrosis by IL-22. World J Gastroenterol 2017; 23: 2002-2011.
[107] Ma Q. Role of Nrf2 in oxidative stress and toxicity. Annu Rev Pharmacol Toxicol 2013; 53: 401-426.
[108] Saha S, Buttari B, Panieri E, Profumo E and Saso L. An overview of Nrf2 signaling pathway and its role in inflammation. Molecules 2020; 25: 5474.
[109] Edeas M, Attaf D, Mailfert AS, Nasu M and Joubet R. Maillard reaction, mitochondria and oxidative stress: potential role of antioxidants. Pathol Biol (Paris) 2010; 58: 220-5.
[110] Kim J, Cha YN and Surh YJ. A protective role of nuclear factor-erythroid 2-related factor-2 (Nrf2) in inflammatory disorders. Mutat Res 2010; 690: 12-23.
[111] Wang R, Song F, Li S, Wu B, Gu Y and Yuan Y. Salvianolic acid A attenuates CCl4-induced liver fibrosis by regulating the PI3K/AKT/mTOR, Bcl-2/Bax and caspase-3/cleaved caspase-3 signaling pathways. Drug Des Devel Ther 2019; 13: 1889-1900.
[112] Mazhari S, Gitiara A, Baghaei K, Hatami B, Rad RE, Asadirad A, Joharchi K, Tokhanbigli S, Hashemi SM, Łos MJ, Aghdaei HA, Zali MR and

Ghavami S. Therapeutic potential of bone marrow-derived mesenchymal stem cells and imatinib in a rat model of liver fibrosis. Eur J Pharmacol 2020; 882: 173263.

[113] Khalil MR, El-Demerdash RS, Elminshawy HH, Mehanna ET, Mesbah NM and Abo-Elmatty DM. Therapeutic effect of bone marrow mesenchymal stem cells in a rat model of carbon tetrachloride induced liver fibrosis. Biomed J 2021; 44: 598-610.

[114] Johnson A and DiPietro LA. Apoptosis and angiogenesis: an evolving mechanism for fibrosis. FASEB J 2013; 27: 3893-901.

[115] Wang R, Wang J, Song F, Li S and Yuan Y. Tanshinol ameliorates CCl4-induced liver fibrosis in rats through the regulation of Nrf2/HO-1 and NF-κB/IκBα signaling pathway. Drug Des Devel Ther 2018; 12: 1281-1292.